CHyPS: An MFEM-Based Material Response Solver for Hypersonic Thermal Protection Systems

April 26, 2022
FEM@LLNL Seminar Series

Robert Chiodi
Center for Hypersonics & Entry Systems Studies
University of Illinois at Urbana-Champaign

Challenges of Hypersonic Flight

Hypersonic flight leads to a wealth of technical challenges

- Speeds exceeding 4,000 miles per hour
- Surface temperatures exceeding that of the sun
- Communication blackout due to gas ionization
- Vehicle guidance and control
- … and many more

X-51 Waverider (Mach 5)

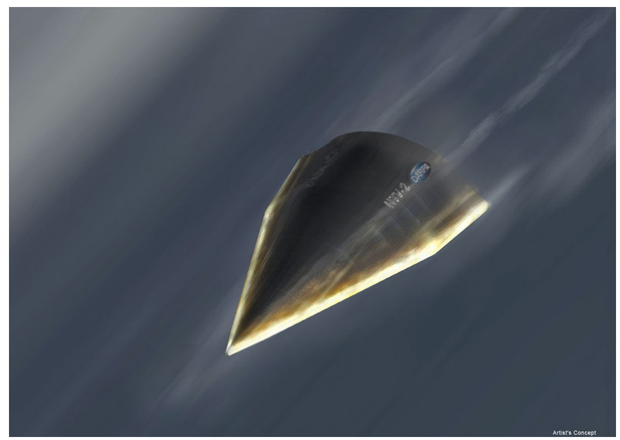

HTV-2 (Mach 20+)

Stardust (Mach 43)

SCRAMJET — Tactical Boost Glide — Reentry Capsule

Center for Hypersonics and Entry-Systems Studies

High-Temperature Materials

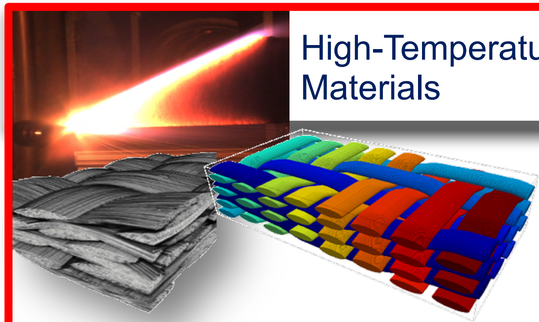

High-Enthalpy Wind Tunnels

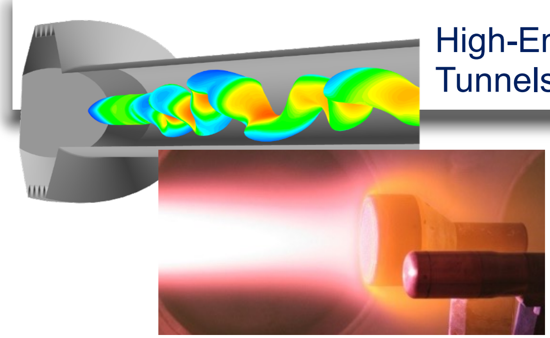

Guidance, Navigation & Control

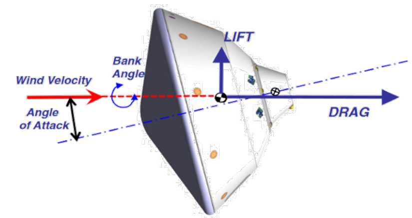

Aerosciences

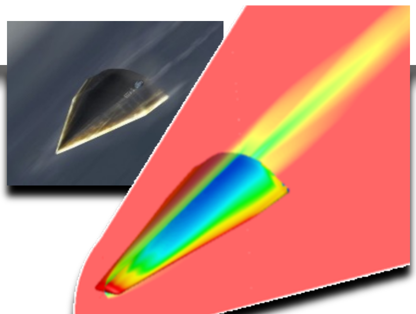

Machine Learning & UQ

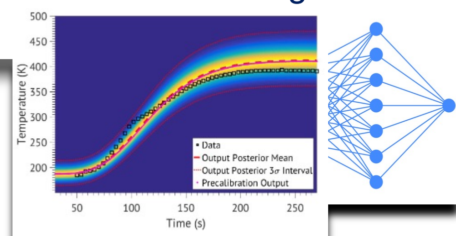

Propulsion

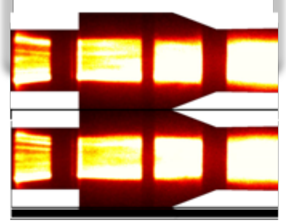

Optical Diagnostics

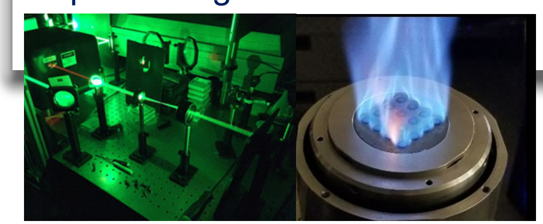

Detection &Tracking

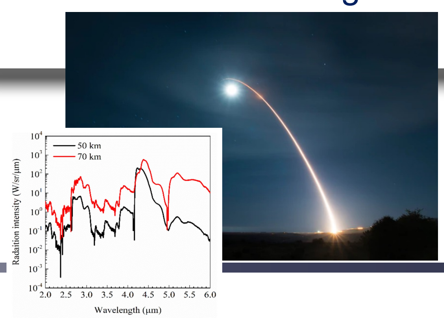

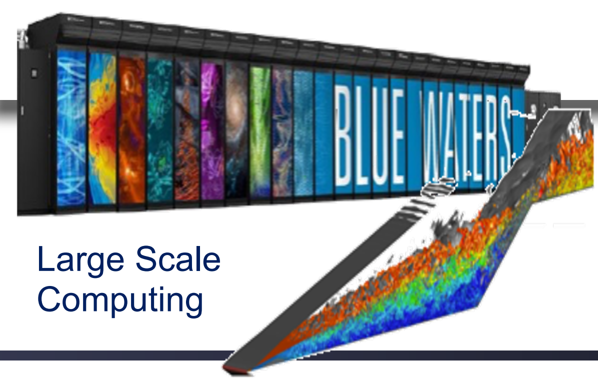

Large Scale Computing

CHESS
CENTER FOR HYPERSONICS & ENTRY SYSTEMS STUDIES

Material Response during Hypersonic Flight

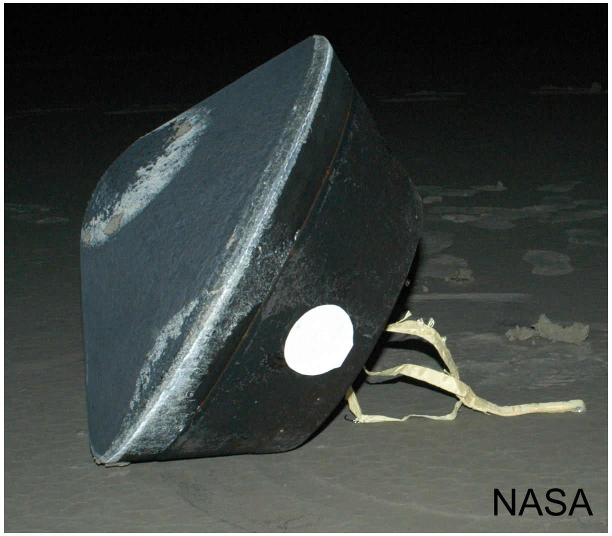

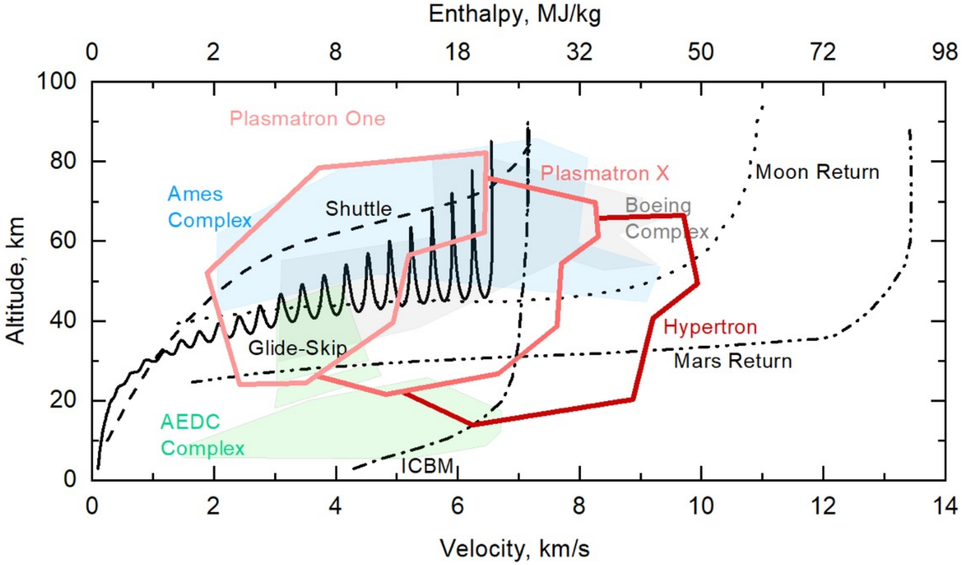

CHESS Experimental Capabilities

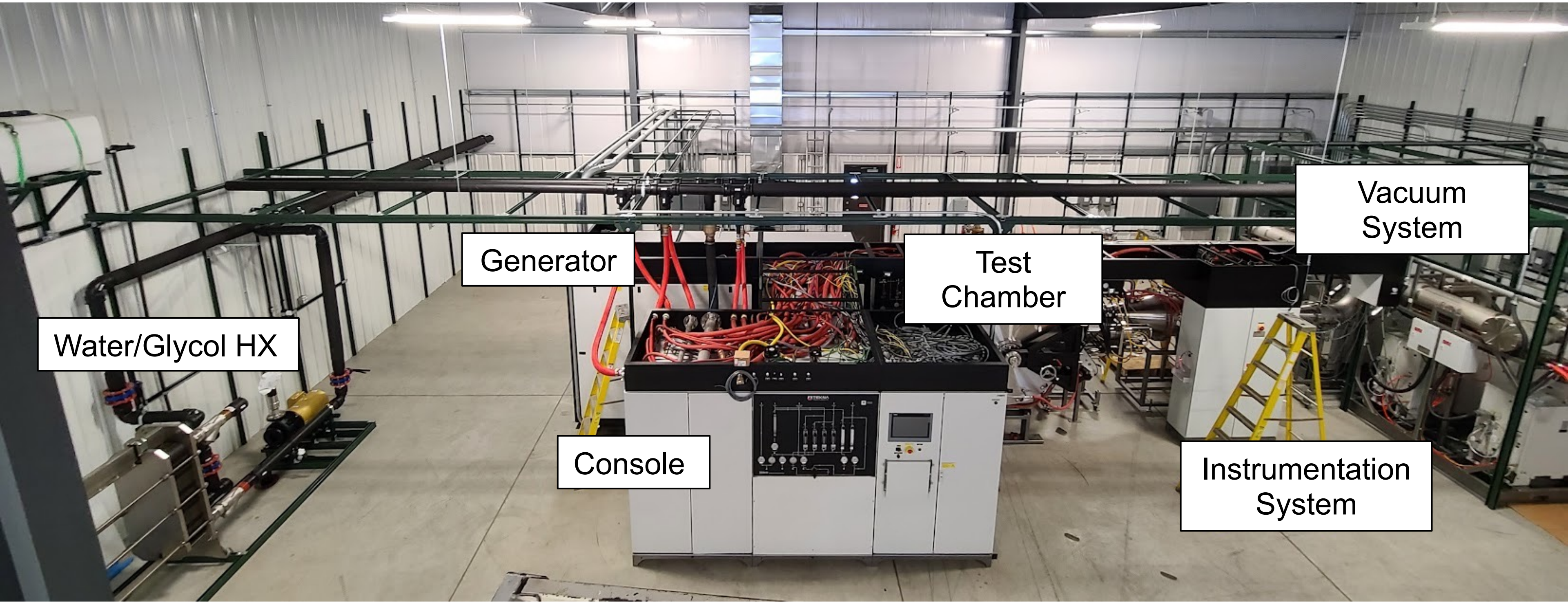

Newly completed Plasmatron-X

CHESS Computational Capabilities

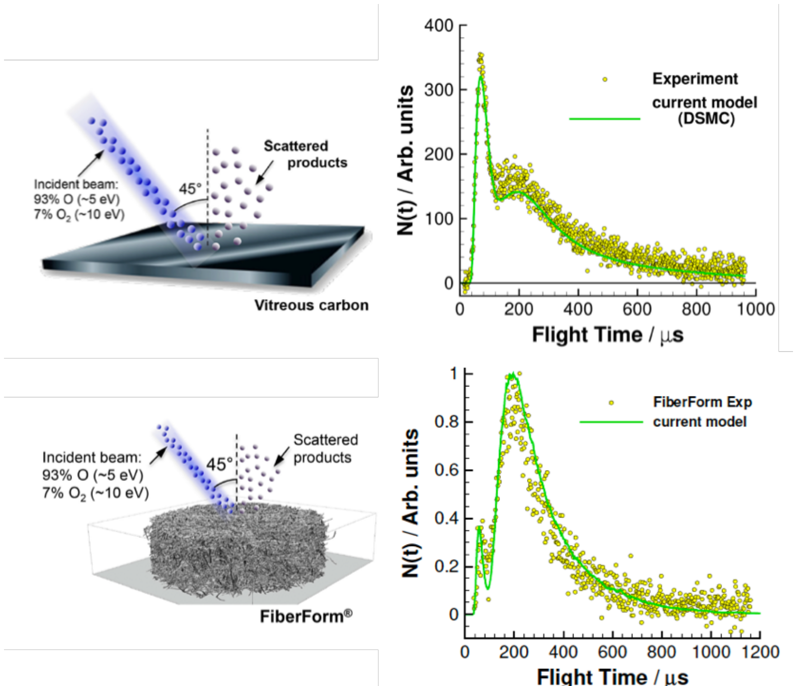

DOE SPARTA DSMC

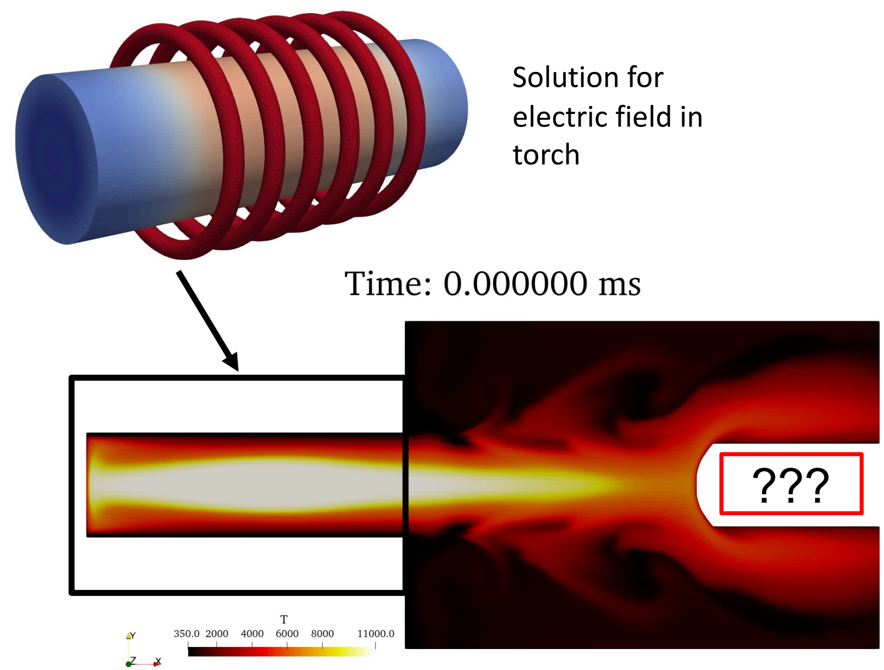

Time-accurate simulation of a Plasmatron facility

My Background is not in FEM…

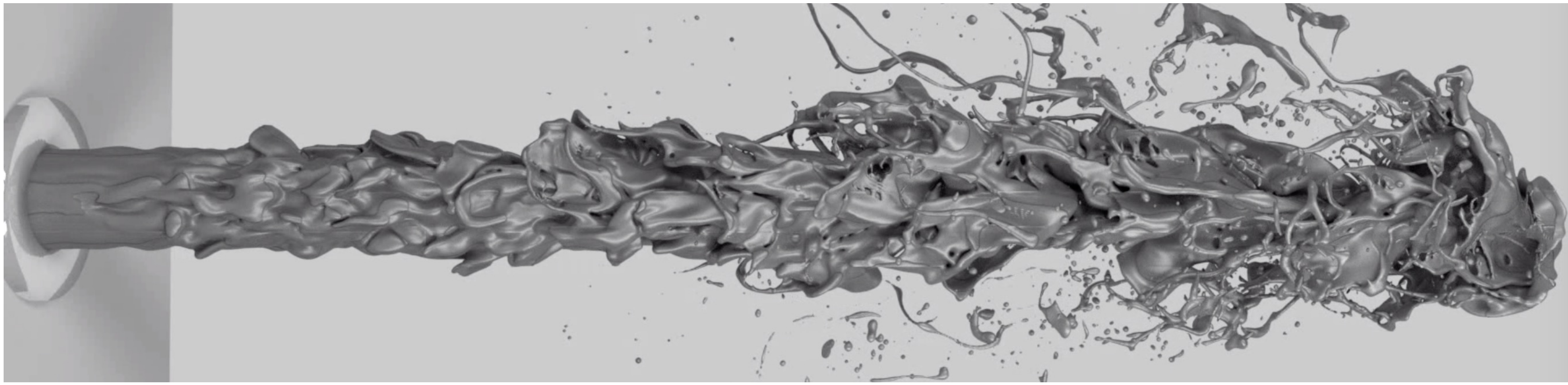

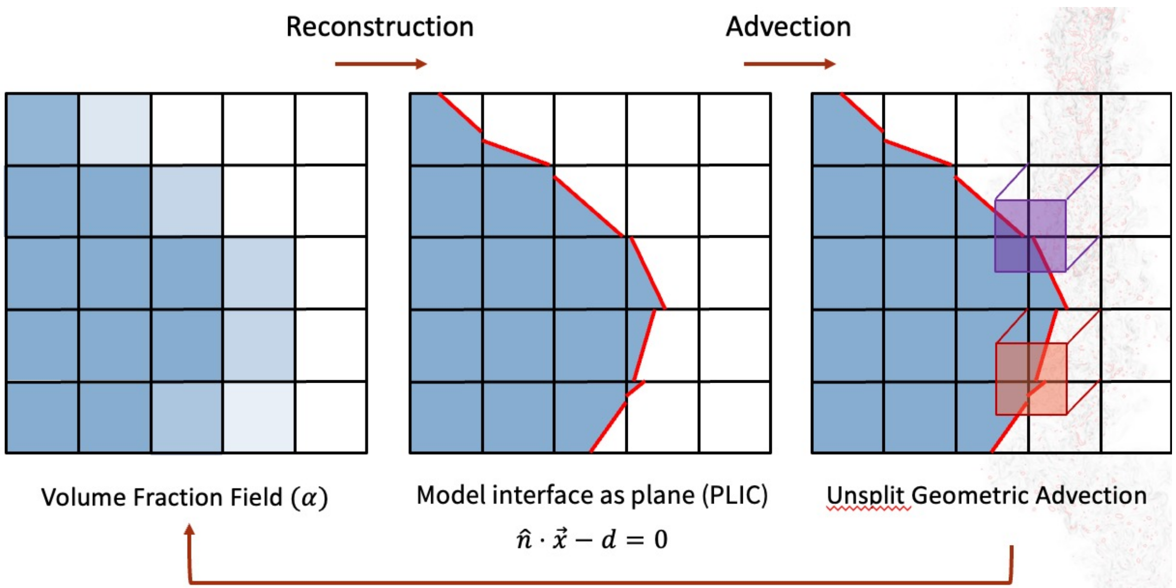

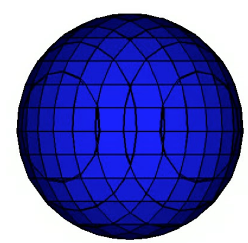

Requirements for a New Material Response Tool

Goal: A state of the art material response solver that can perform full-vehicle simulations and readily couple to external solvers to add additional physics

Tool features required for full-vehicle simulation

- Scalability to large problems and core counts
- Faithful representation of vehicle geometry features
- Robustness to low quality meshes
- Correct level of abstraction and flexibility for physical model

Targeting cases where coupled response is important

- Material response of control surfaces and thin-ablators
- Boundary layer stability and transition on ablating surfaces
- Development of small-dimension models for guidance and control

Macroscopic phenomenology | Macroscopic illustration | Microscopic illustration

Hypersonic flow

Long distance effects
- Radiation

Material-flow coupling
- Boundary layer transfers (heat and mass)
- Recombination/catalicity
- Ablation (oxidation, sublimation, spallation)

Material response

Interface phenomena: Heat and mass balance (1),
Subsurface phenomena
- In-depth ablation (3)
- Penetration of radiation (3)
- Gas flow entering into the material (3)

- Conduction heat transfer (1)
- Radiation heat transfer (empirical: 1, modeled: 3)
- Finite rate chemistry of the pyrolysis gases (3)
- Coking (3)

- Multicomponent diffusion (3)
- Convective transport (Darcy: 2, Klinkenberg: 3)
- Charring process (evolution of the density: 1, porosity: 2, tortuosity: 3, permeability: 2, effective conductivity: 1, effective surface area: 3)

- Phenolic-decomposition product (3)
- Phenolic-decomposition rate (1)

1 : in all material response models (type 1)
2 : in some material response models (type 2)
3 : in analysis material response models (type 3)

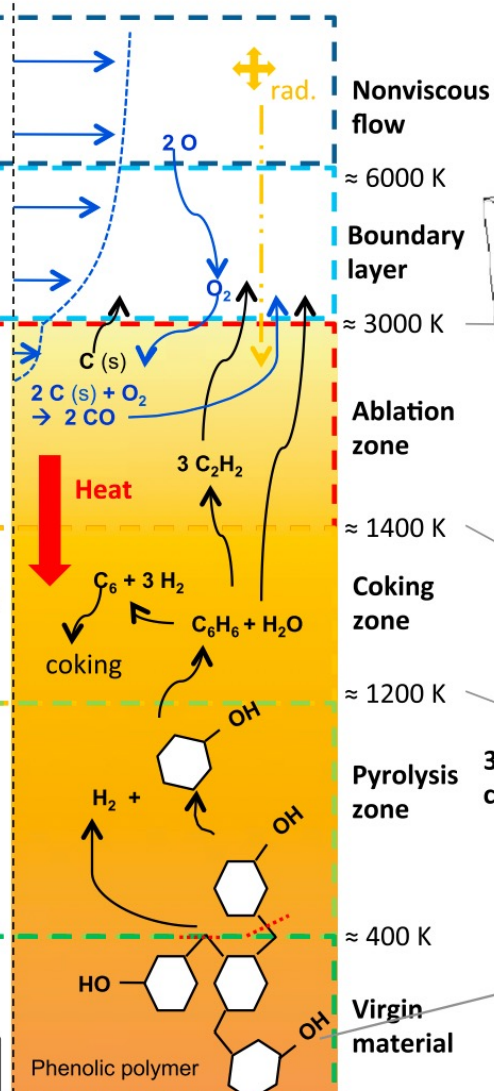

Chemistry mechanisms (simplified illustration)

Gas/surface interactions in porous fibrous media (3):
- in-depth ablation
- erosion
- in-depth recombination
- coupled heat transport (diffusion, convection, radiation)

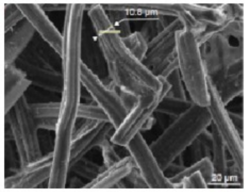

Scanning electron microscopy (SEM) : Carbon preform

3-D simulation of the ablation of a carbon/phenolic composite [Lachaud [6]]

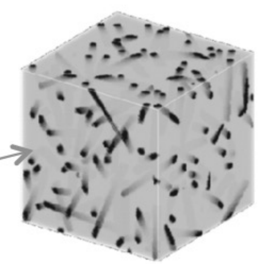

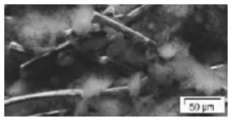

SEM: carbon/phenolic (virgin) [Stackpoole, 2008]

3-D reconstitution of a carbon/phenolic composite

Governing Physics

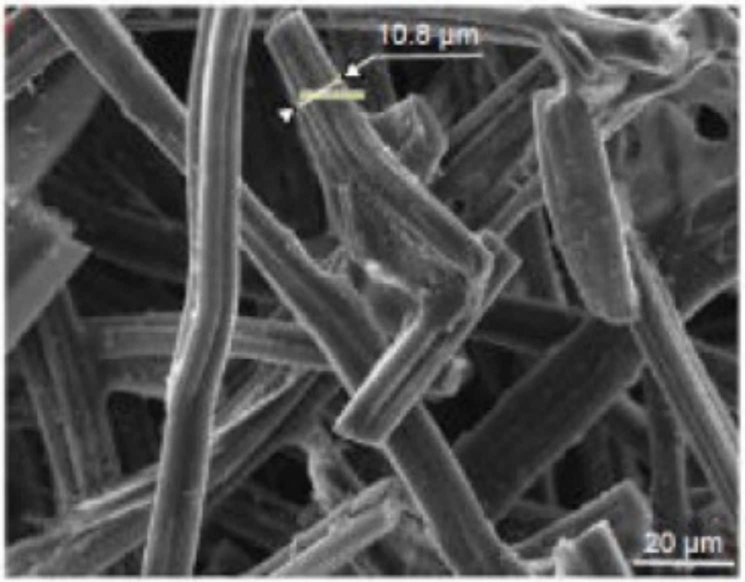

SEM of carbon preform
prior to phenolic impregnation [1]

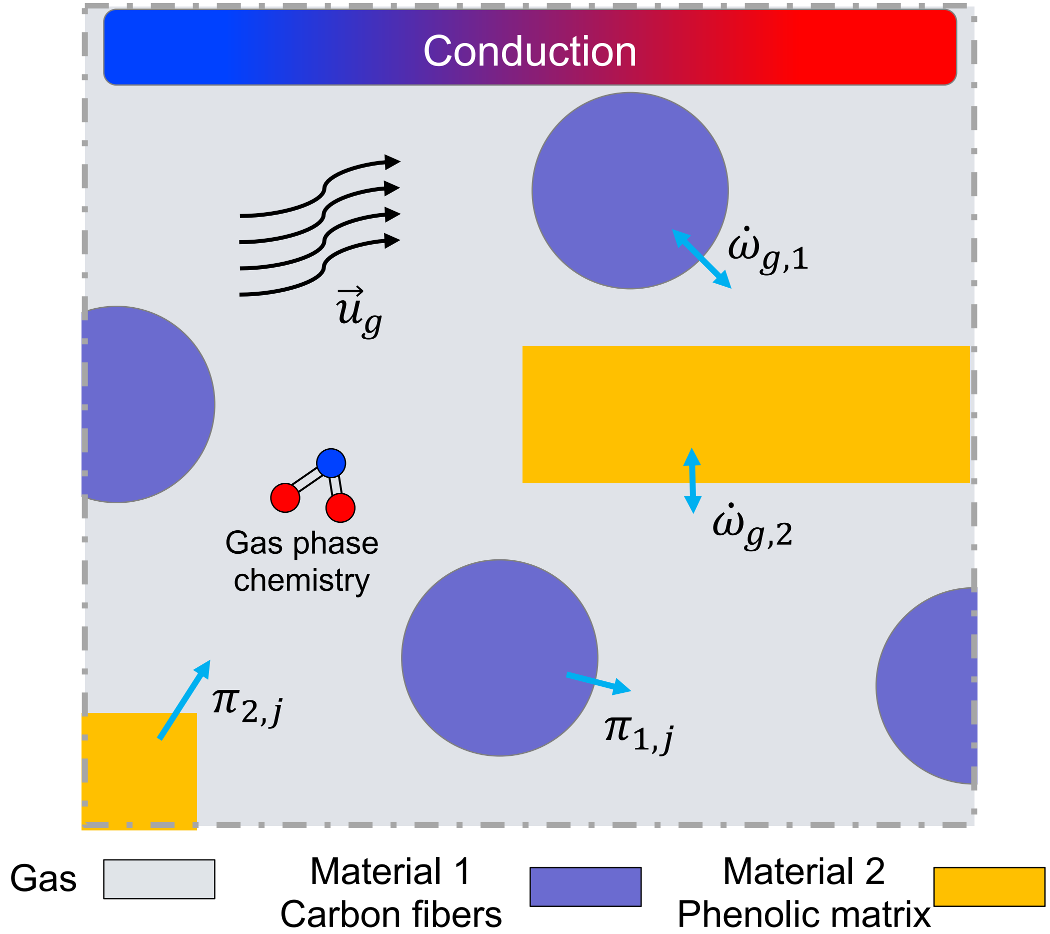

[1] Lachaud et al. IJHMT. 2015

Governing Physics

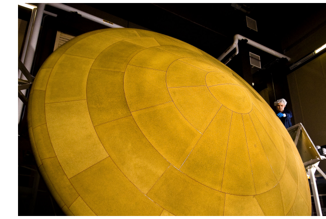

Gas properties

Volume fraction ϵ_g
Pressure P_g
Enthalpy h_g
Density ρ_g
Viscosity μ_g

Material properties ($i \in [1, N_p]$)

Volume fraction ϵ_i
Density ρ_i
Specific heat $c_{p,i}$
Enthalpy h_i
Pyrolysis specie production $\pi_{i,k}$

Bulk properties

Temperature T (thermal equilibrium)
Conductivity κ
Permeability K

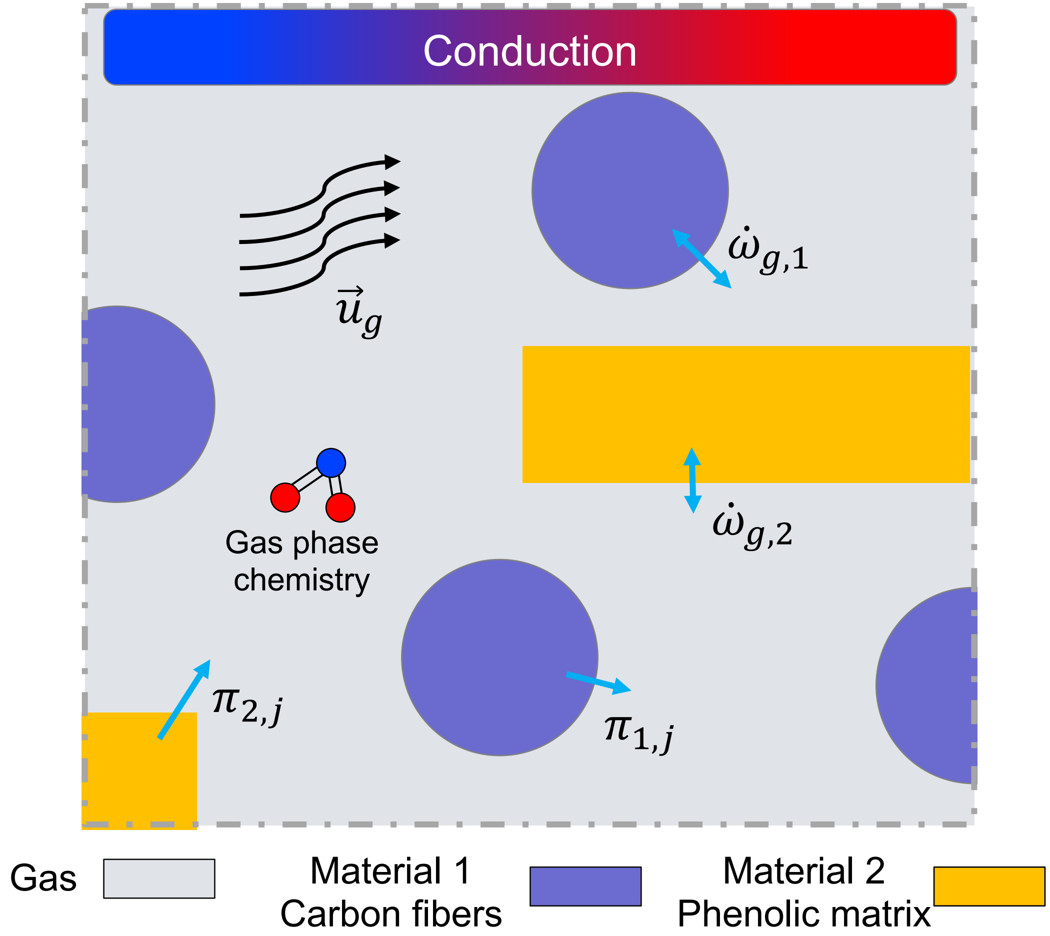

[1] Lachaud et al. IJHMT. 2015

Volume-Averaging over a Representative Elementary Volume

Smallest volume that is representative of the bulk properties of the whole

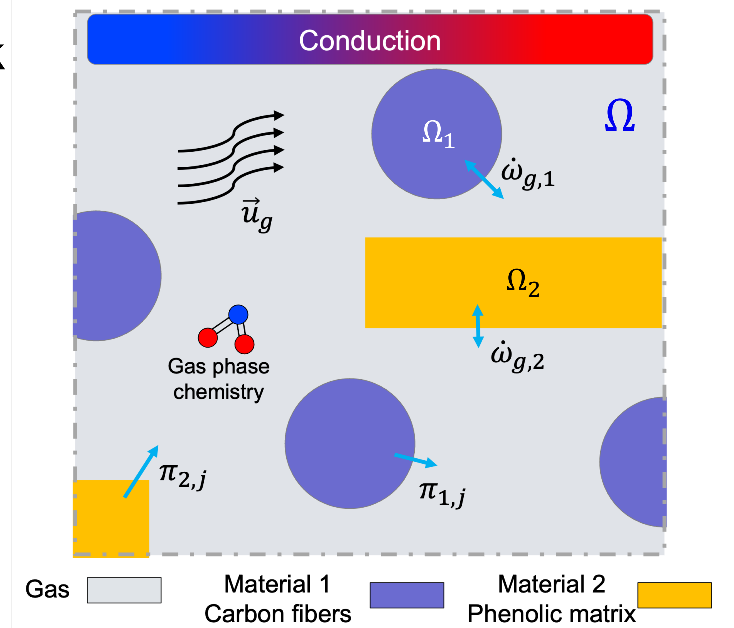

Phase indicator functions:

$$H(\vec{x}) = \begin{cases} 1, & \vec{x} \in \text{phase} \\ 0, & \vec{x} \notin \text{phase} \end{cases}$$

For a fiber/matrix composite, three total phases

Volume fraction:

$$\epsilon_i = \frac{\int_\Omega H_i(\vec{x})\, d\vec{x}}{\int_\Omega d\vec{x}} \text{ or } \epsilon_i = \frac{\int_{\Omega_i} d\vec{x}}{\int_\Omega d\vec{x}}$$

Average solid density:

$$\rho_s = \frac{\sum_{i \in N_p} \int_{\Omega_i} \rho_i\, d\vec{x}}{\int_\Omega d\vec{x}} = \sum_{i \in N_p} \epsilon_i\, \rho_i$$

CHESS
CENTER FOR HYPERSONICS & ENTRY SYSTEMS STUDIES

Governing Equations

Solid mass conservation:

$$\frac{\partial \epsilon_i \rho_i}{\partial t} = -\sum_{k\,\in\,[1,N_{sp}]} \pi_{i,k}$$

Gas mass conservation equation with ideal gas law and Darcy's law assumption

Gas mass/momentum conservation:

$$\frac{\partial}{\partial t}\left(\frac{\epsilon_g M P_g}{RT}\right) - \nabla \cdot \left(\frac{P_g M}{RT\mu} K \nabla P_g\right) = \sum_{\substack{i\,\in\,[1,N_p],\\ k\,\in\,[1,N_{sp}]}} \pi_{i,k}\,, \qquad \vec{u}_g = -\frac{K}{\epsilon_g \mu}\nabla P_g$$

Energy conservation:

$$\left(\sum_{i\,\in\,[1,N_p]} \epsilon_i \rho_i c_{p,i}\right)\frac{\partial T}{\partial t} - \nabla \cdot \kappa \nabla T = -\sum_{i\,\in\,[1,N_p]} h_i \frac{\partial \epsilon_i \rho_i}{\partial t} - \frac{\partial\left(\epsilon_g \rho_g h_g - \epsilon_g P_g\right)}{\partial t} - \nabla \cdot (\epsilon_g \rho_g h_g \vec{u}_g)$$

Pyrolysis chemistry:

$$\frac{\partial X_{i,j}}{\partial t} = \left(1 - X_{i,j}\right)^{m_{i,j}} T^{n_{i,j}} A_{i,j} \exp\left(-\frac{\mathrm{E}_{i,j}}{RT}\right), \qquad \pi_{i,k} = \sum_{j\,\in\,[1,P_i]} \zeta_{i,j,k}\epsilon_{i,0}\rho_{i,0}F_{i,j}\frac{\partial X_{i,j}}{\partial t}$$

CHESS
CENTER FOR HYPERSONICS & ENTRY SYSTEMS STUDIES

[1] Lachaud et al. IJHMT. 2017

Ablative Boundary Condition

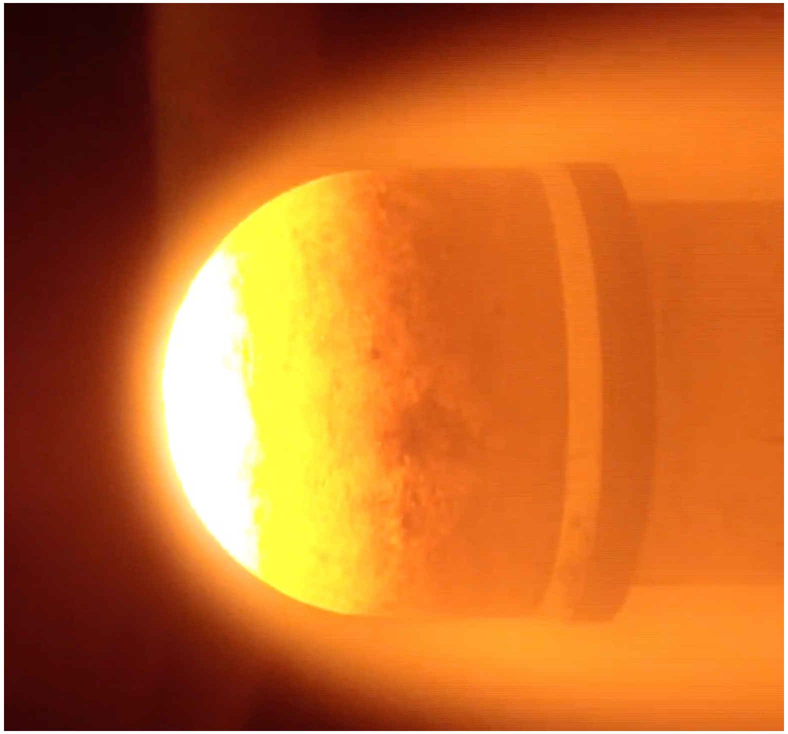

Ablative Boundary Condition

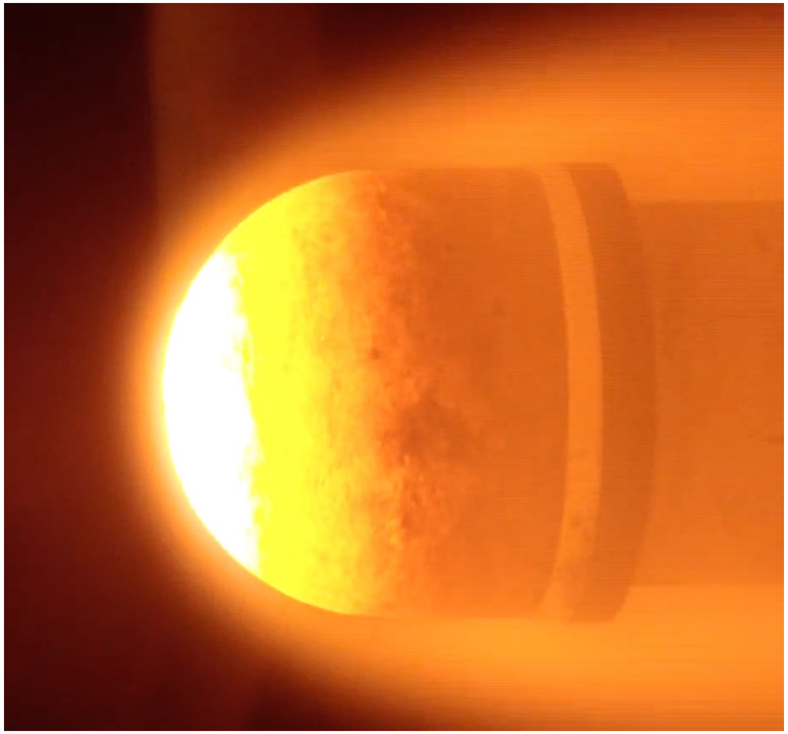

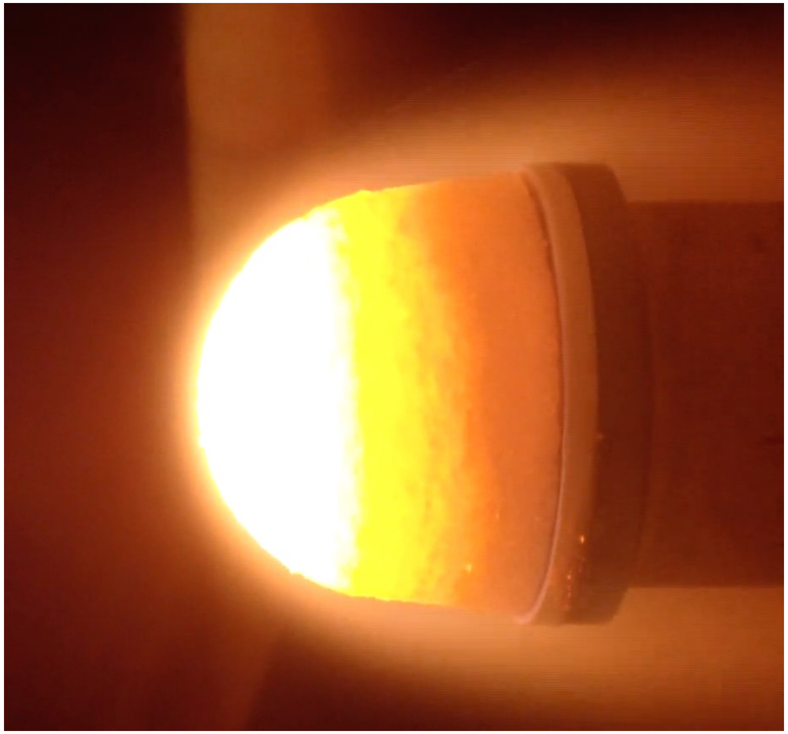

Ablative Boundary Condition

Ablative surface boundary condition from local equilibrium assumption

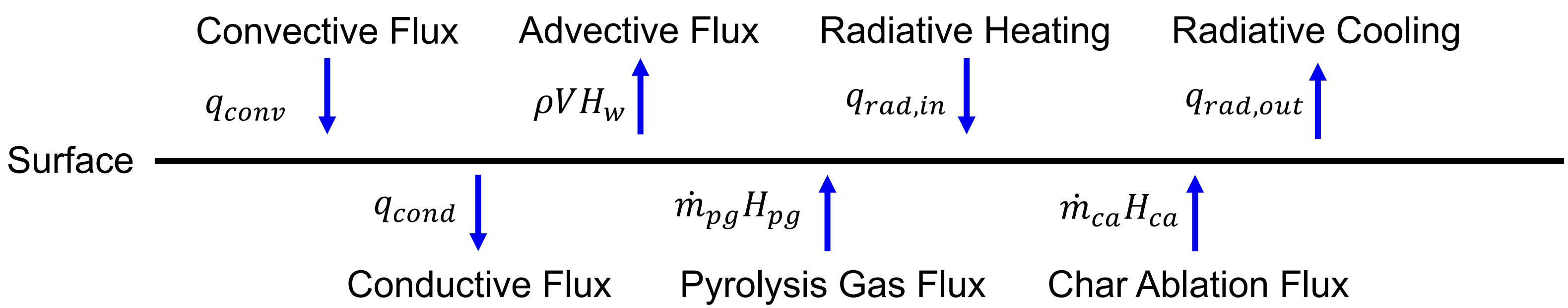

Provides Neumann boundary condition (heat flux) for energy equation

$$q_{cond} = q_{conv} - \rho V H_w + q_{rad,in} - q_{rad,out} + \dot{m}_{pg} H_{pg} + \dot{m}_{ca} H_{ca}$$

B' table is used to compute $\dot{m}_{ca}$ and H_w as a function of $f\left(P, T, \dot{m}_{pg}\right)$

$\dot{m}_{ca}$ directly controls the ablative surface recession

[1] Lachaud et al. IJHMT. 2017

Governing Equations - ALE

An Arbitrary Lagrangian Eulerian (ALE) used to allow moving mesh

Employ the conservative direct ALE method of Ivančić et al. 2019[1]

Consider the heat equation $\left.\frac{\partial u}{\partial t}\right|_{\hat{x}} - \alpha\nabla^2 u - \vec{w}\cdot\nabla u = f$ in weak form with backward Euler time-integration

$$\int_{\hat{\Omega}} \hat{\psi}\hat{u}_{n+1}\hat{\mathcal{J}}_{n+1}\,d\hat{x} - \int_{\hat{\Omega}} \hat{\psi}\hat{u}_n\hat{\mathcal{J}}_n\,d\hat{x} + d_{n,n+1}(\hat{u}_{n+1},\hat{\psi}) - b_{n,n+1}(\hat{u}_{n+1},\hat{\psi}) - \mathcal{M}_{n,n+1}(\hat{u}_{n+1},\hat{\psi}) = 0$$

$$d_{n,n+1}(\hat{u}_k,\hat{\psi}) = \Delta t\int_{\hat{\Omega}} \alpha\frac{1}{\hat{\mathcal{J}}_{n,n+1}(\Delta t)}\hat{F}_{n,n+1}(\Delta t)\hat{F}^T_{n,n+1}(\Delta t)\hat{\nabla}\hat{\psi}\cdot\hat{\nabla}\hat{u}_k d\hat{x}$$

$$b_{n,n+1}(\hat{f}_k,\hat{\psi}) = \Delta t\int_{\hat{\Omega}} \hat{\psi}\hat{f}_k\hat{\mathcal{J}}_{n,n+1}(\Delta t)d\hat{x}$$

$$\mathcal{M}_{n,n+1}(\hat{u}_k,\hat{\psi}) = \int_{\hat{\Omega}} \hat{\psi}\left[\int_0^{\Delta t}\hat{F}_{n,n+1}(t)\hat{w}_{n,n+1}(t)dt\right]\hat{\nabla}\hat{u}_k d\hat{x} + \int_{\hat{\Omega}} \hat{\psi}\hat{u}_k\hat{\nabla}\cdot\left[\int_0^{\Delta t}\hat{F}_{n,n+1}(t)\hat{w}_{n,n+1}(t)dt\right]d\hat{x}$$

CHESS
CENTER FOR HYPERSONICS & ENTRY SYSTEMS STUDIES

[1] Ivančić et al., SIAM J. Sci. Comput. 2019

Multi-Stage `BilinearForm`

Created a Multi-Stage BilinearForm to implement the direct ALE method

- Assumes integrating over $t \in [t_o, t_o + \Delta t]$ and known nodal displacement

Integrators are added to specific time-stages of the BilinearForm

- Added independently for each time stage
- Can include both domain and boundary integrators

Each time-stage has an associated `GridFunction` denoting nodal locations

- Nodes set on `Mesh` before building of each time-stage
- References to nodes stored, allowing external update of locations

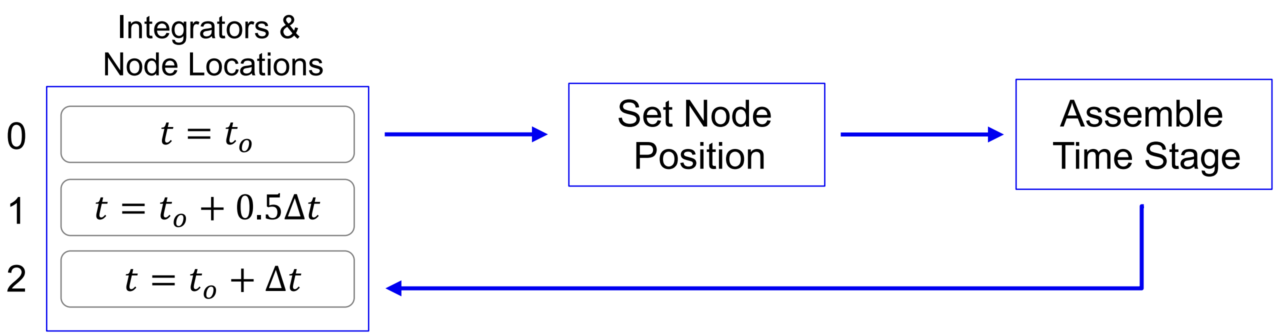

Governing Equations - ALE

$$\partial_t u - 0.1\Delta u = f \text{ in } \Omega(t) \times (0,T),$$
$$u = 0 \text{ on } \partial\Omega(t) \times (0,T),$$
$$u(0) = 16x(1-x)y(1-y) \text{ in } \Omega(0)$$

$$u(x,t) = 16\left(1 + \frac{1}{2}\sin(\pi t)\right)x(1-x)y(1-y)$$

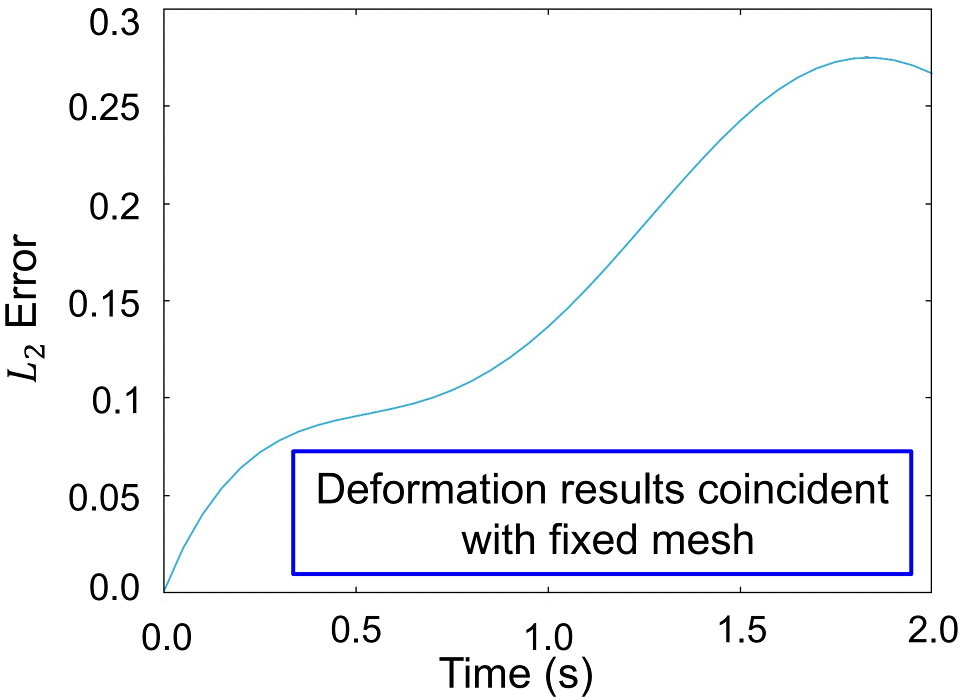

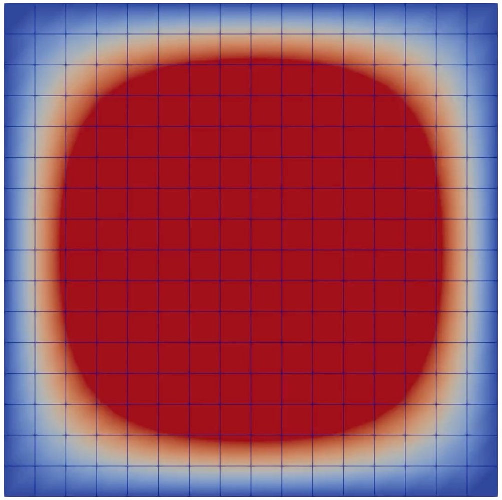

Deformation A

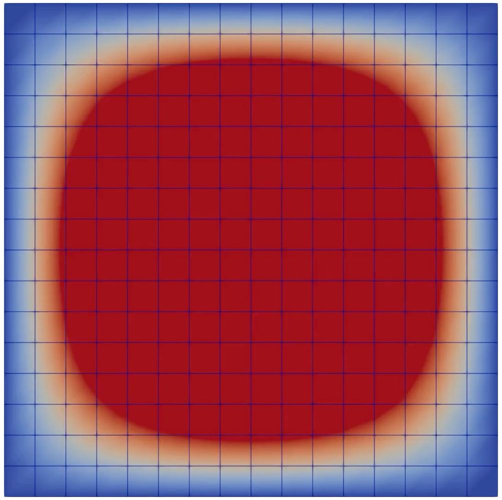

Deformation B

Implementation

Implemented in the Coupled Hypersonic Protection System (CHyPS) Simulator

Discontinuous Galerkin spatial discretization via MFEM library [1]

Crank-Nicolson, Forward Euler, and Backward Euler time integration available

- Custom time-integration currently used, would like to return to MFEM ODE solvers

Tensor properties for conductivity and permeability

Coupling to external solvers using the preCICE library

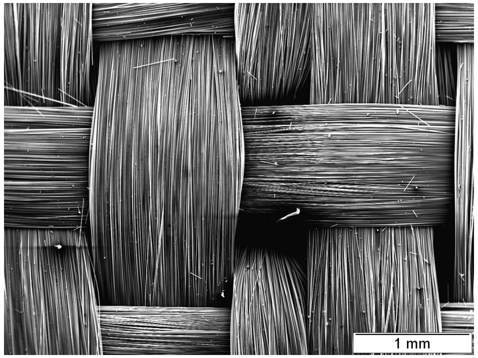

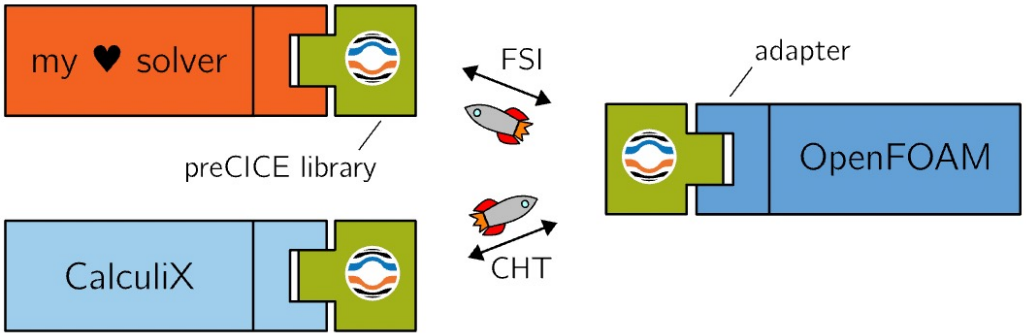

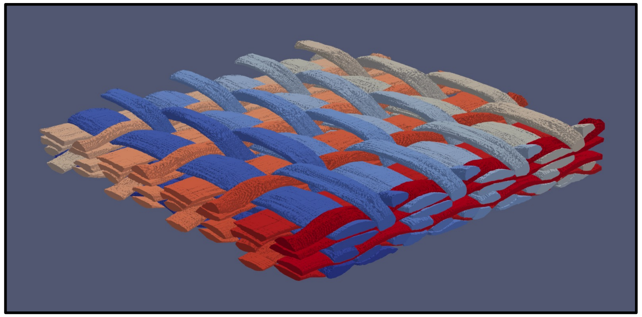

[1] mfem.org
[2] precice.org

Ablation Test Case Series

Series of test cases developed over the last decade for code comparison

- Makes available open-results for a field dominated by national defense
- Feature Theoretical Ablative Composite for Open Testing (TACOT)
- Provide gradual increase in physical and computational complexity

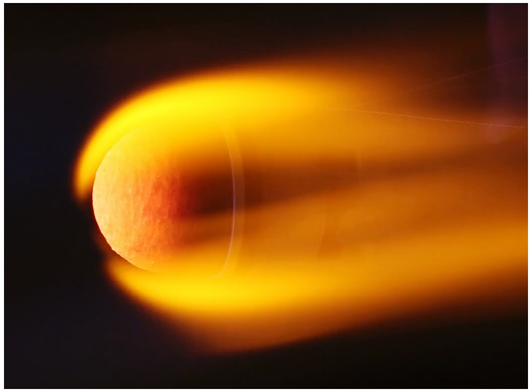

Ablation Test Case 2

- Mimics the 1D heating of a sample in an arc jet facility
- Will compare against the Porous-Material Analysis Toolbox Based on OpenFOAM (PATO)

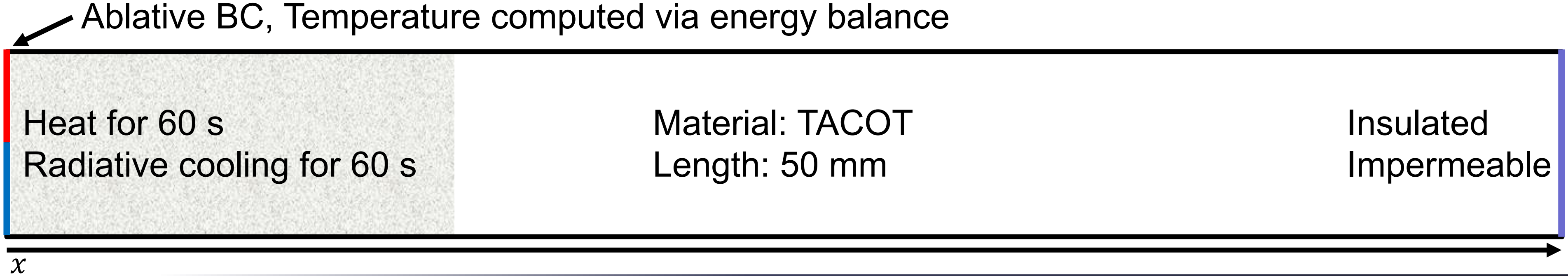

[1] Lachaud et al. 5th Ablation Workshop. 2012

Ablation Test Case 2.3

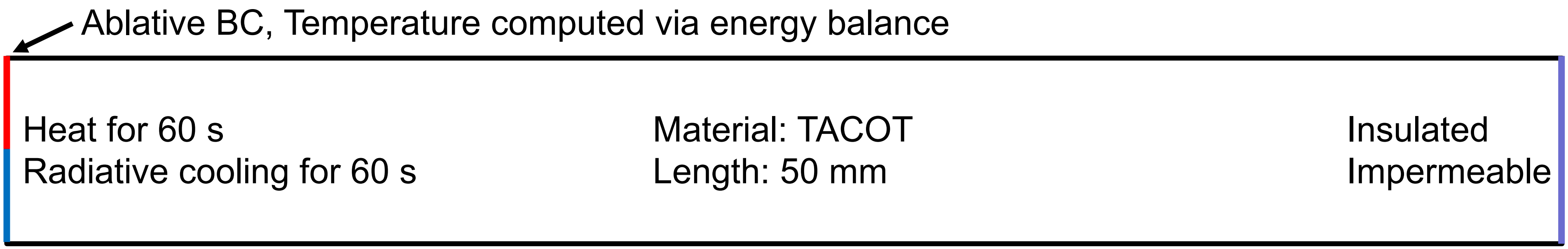

[1] Lachaud et al. 5th Ablation Workshop. 2012

Ablation Test Case 2.3

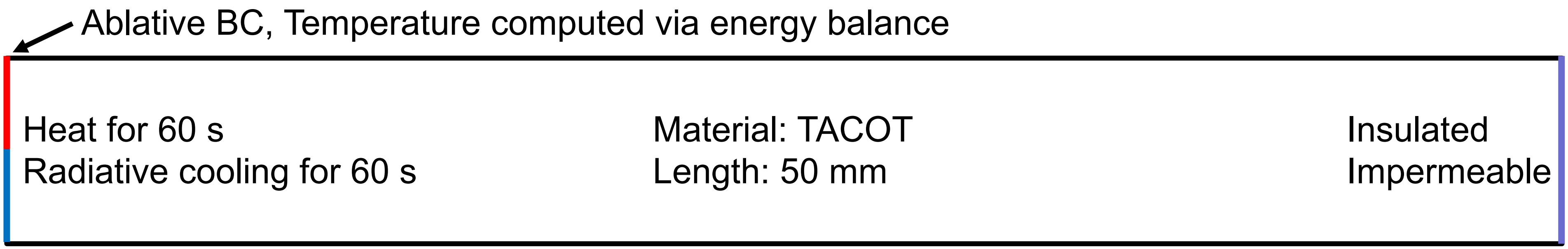

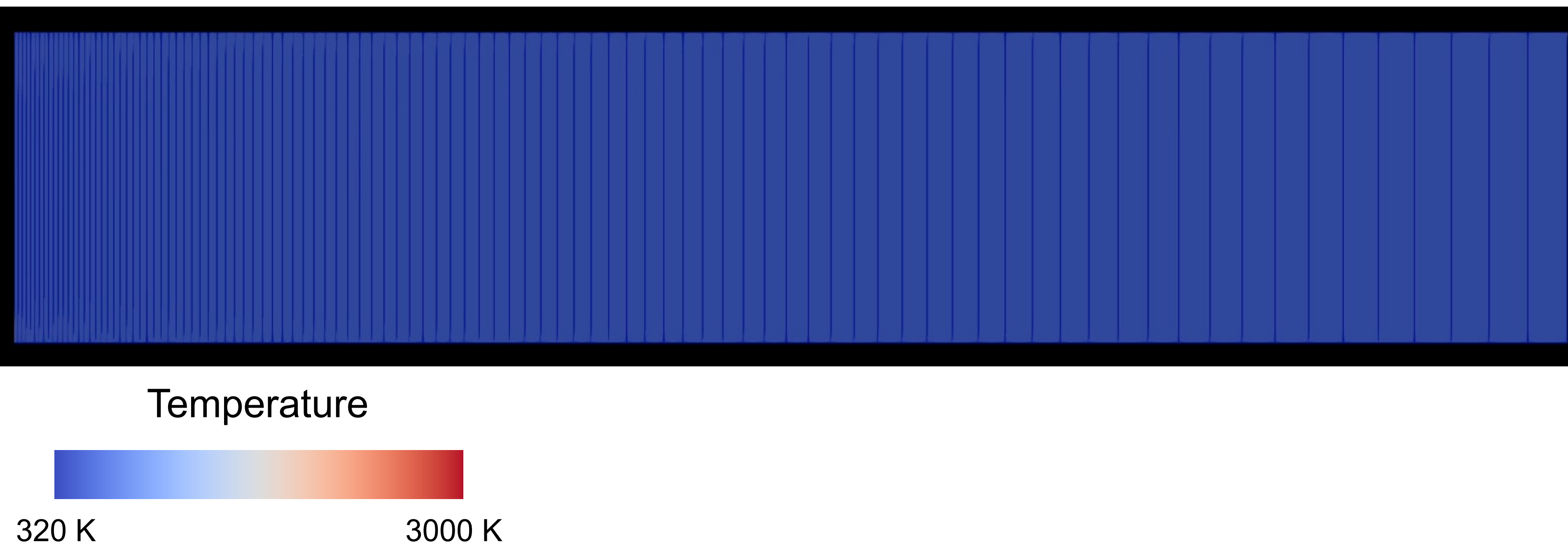

[1] Lachaud et al. 5th Ablation Workshop. 2012

Ablation Test Case 2.3

Ablative BC, Temperature computed via energy balance

Heat for 60 s
Radiative cooling for 60 s

Material: TACOT
Length: 50 mm

Insulated
Impermeable

Probe	x (mm)
Surface	0.0
1	1.0
2	2.0
3	4.0
4	8.0
5	12.0
6	16.0
7	24.0

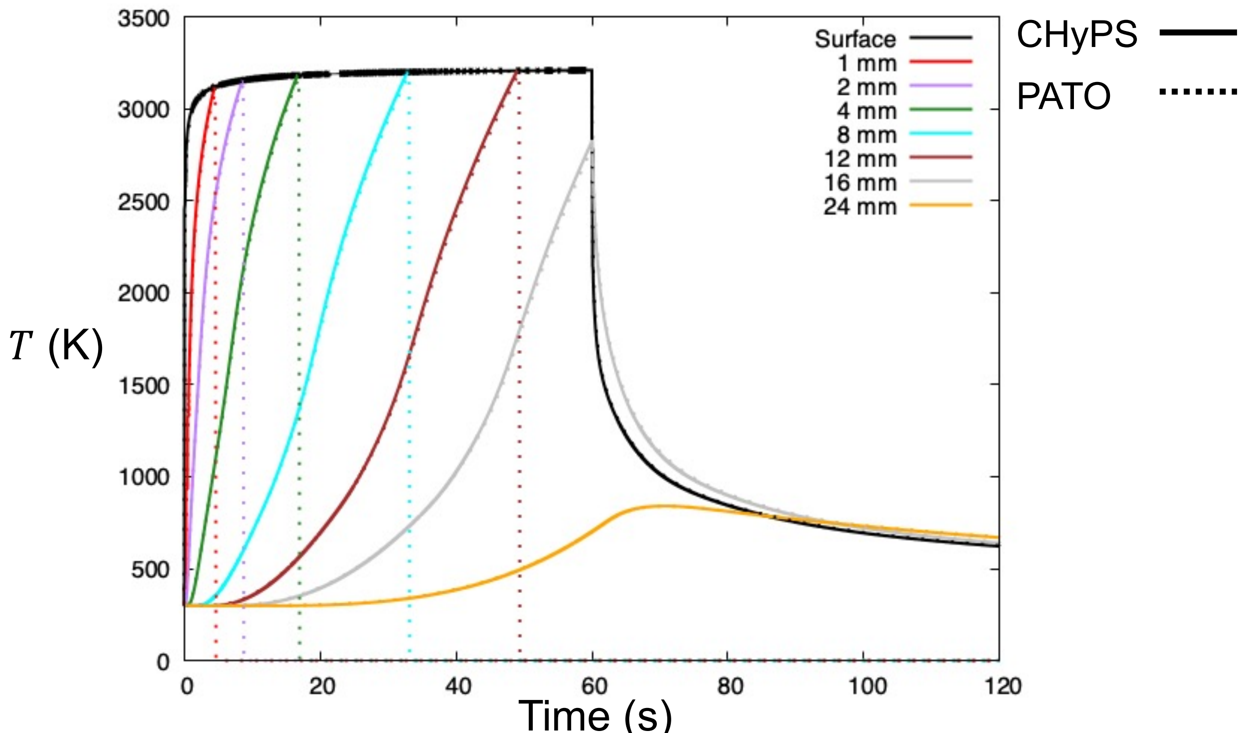

[1] Lachaud et al. 5th Ablation Workshop. 2012

Ablation Test Case 2.3

Ablative BC, Temperature computed via energy balance

Heat for 60 s
Radiative cooling for 60 s

Material: TACOT
Length: 50 mm

Insulated
Impermeable

Probe	x (mm)
Surface	0.0
1	1.0
2	2.0
3	4.0
4	8.0
5	12.0
6	16.0
7	24.0

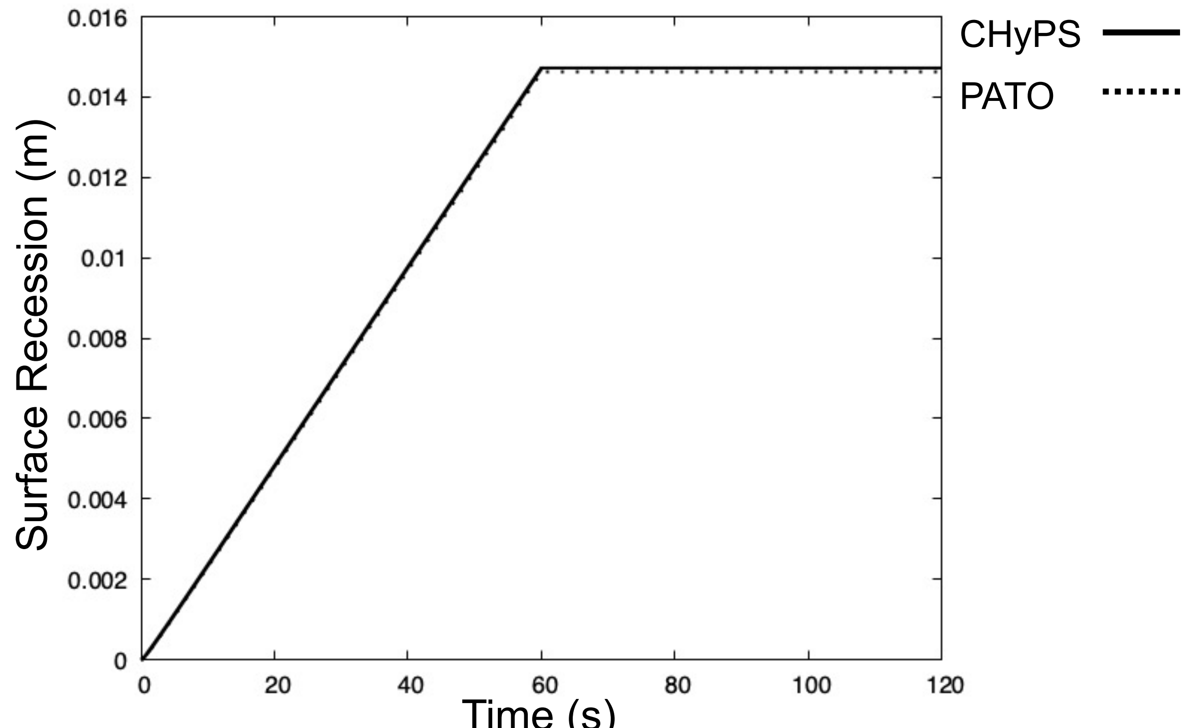

[1] Lachaud et al. 5th Ablation Workshop. 2012

Ablation Test Case 2.3

Ablative BC, Temperature computed via energy balance

Heat for 60 s
Radiative cooling for 60 s

Material: TACOT
Length: 50 mm

Insulated
Impermeable

Probe	x (mm)
Surface	0.0
1	1.0
2	2.0
3	4.0
4	8.0
5	12.0
6	16.0
7	24.0

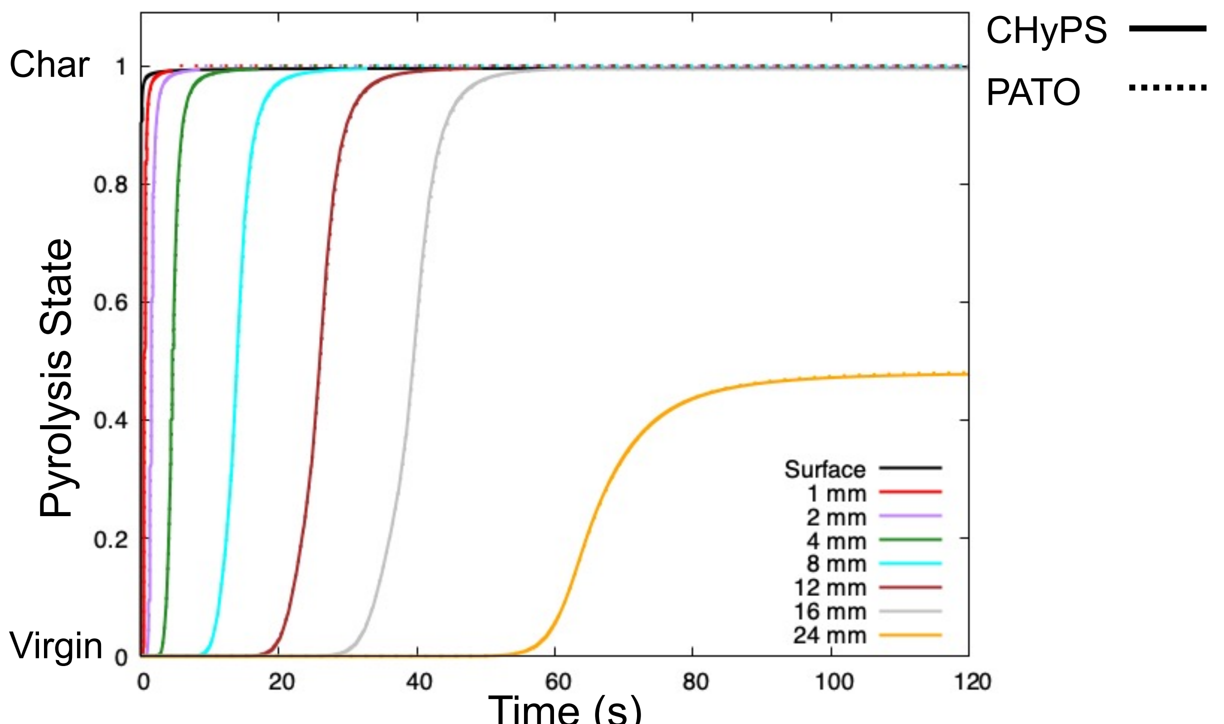

[1] Lachaud et al. 5th Ablation Workshop. 2012

Axisymmetric Mini Arc Jet Case

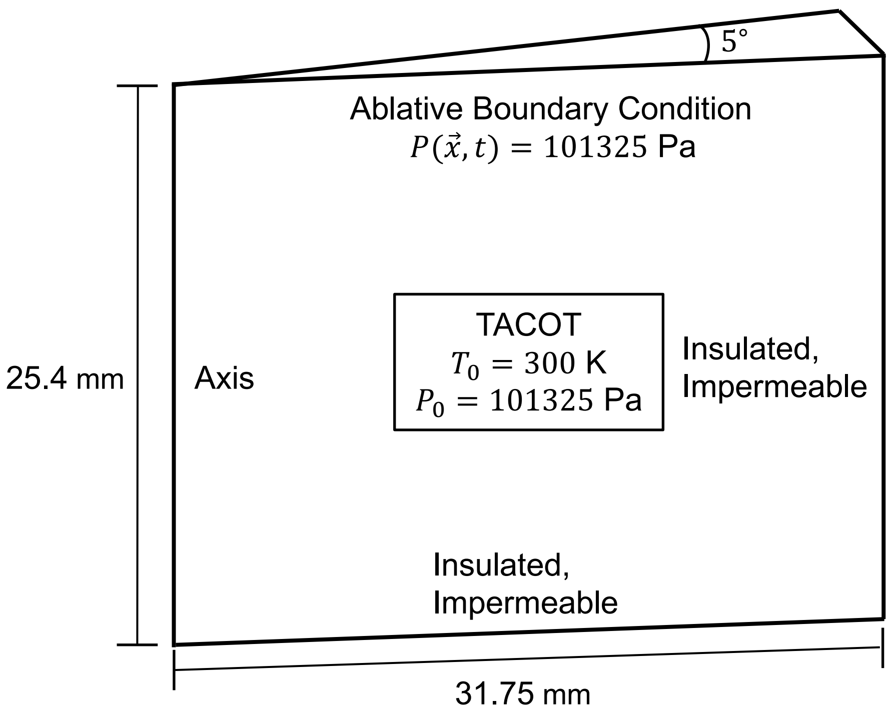

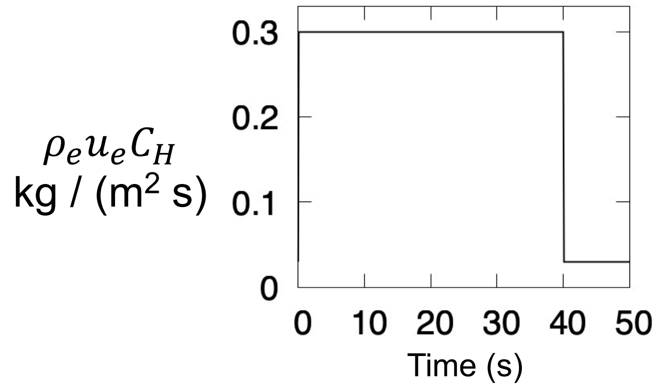

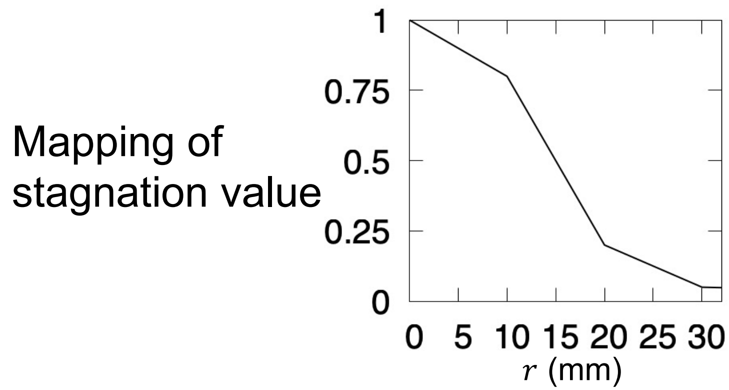

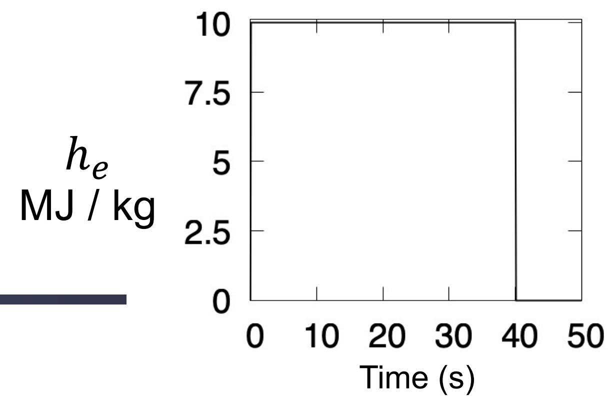

<u>CHyPS</u>
20 elements along radius
50 elements along height
DG, $p = 1$ polynomials

<u>PATO</u>
40 elements along radius
100 elements along height
Finite-volume method

Axisymmetric Mini Arc Jet Case

Temperature

Gas Pressure

CHESS
CENTER FOR HYPERSONICS & ENTRY SYSTEMS STUDIES

Axisymmetric Mini Arc Jet Case

$\boxed{t = 20 \text{ s}}$

Pyrolysis State

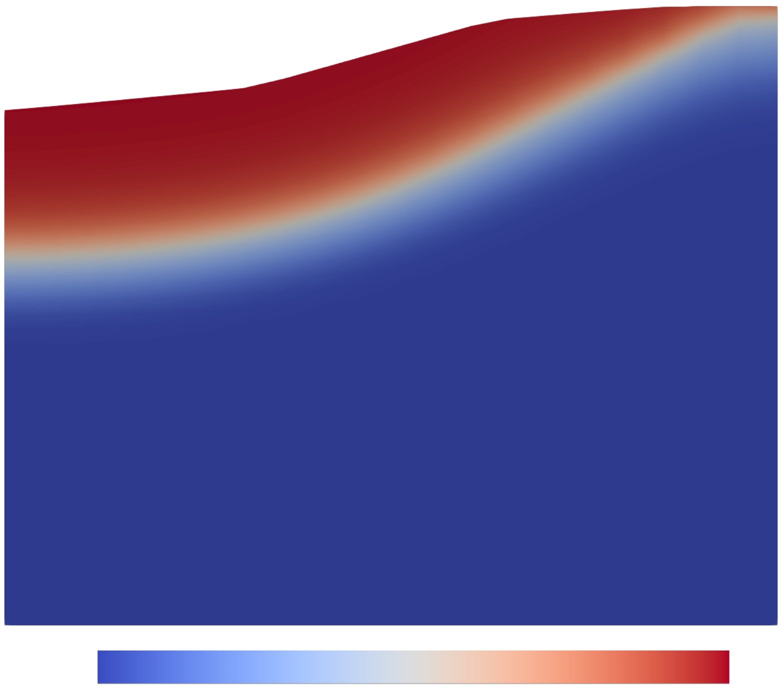

Gas Pressure and Velocity

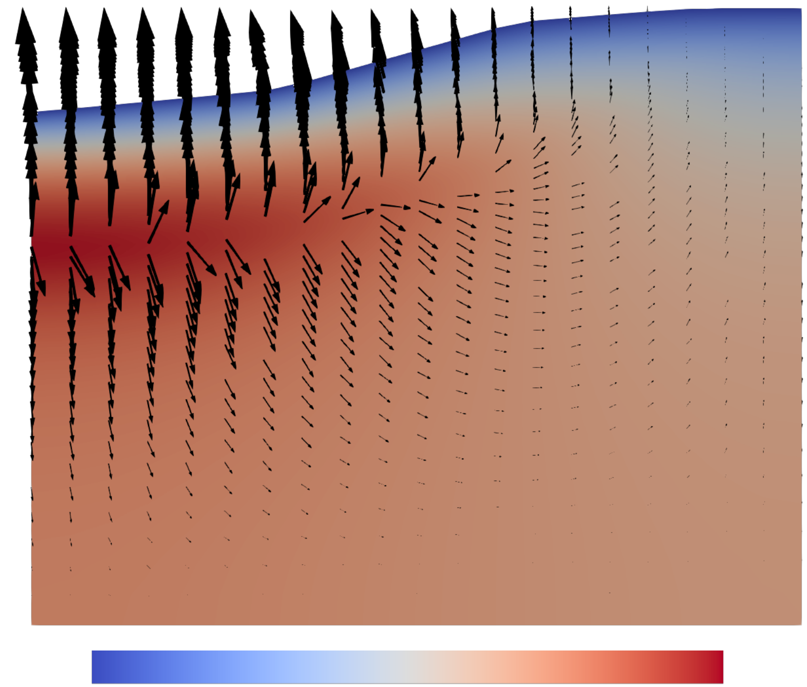

Axisymmetric Mini Arc Jet Case

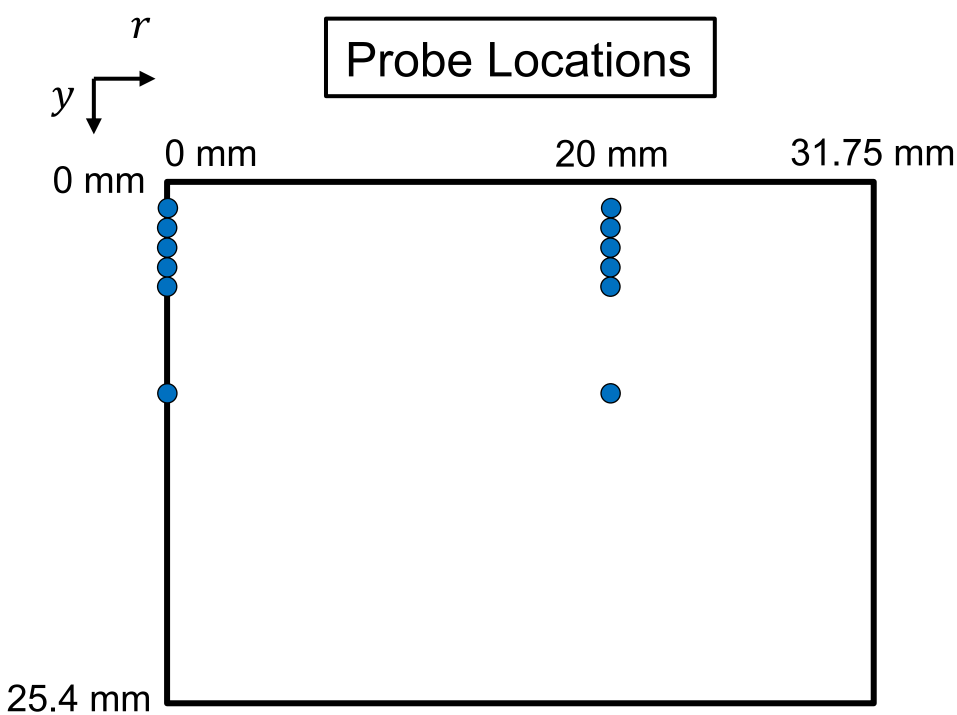

Probe	r (mm)	y (mm)	Probe	r (mm)	y (mm)
1	0	1.4	7	20	1.4
2	0	2.4	8	20	2.4
3	0	3.4	9	20	3.4
4	0	4.4	10	20	4.4
5	0	5.4	11	20	5.4
6	0	10.4	12	20	10.4

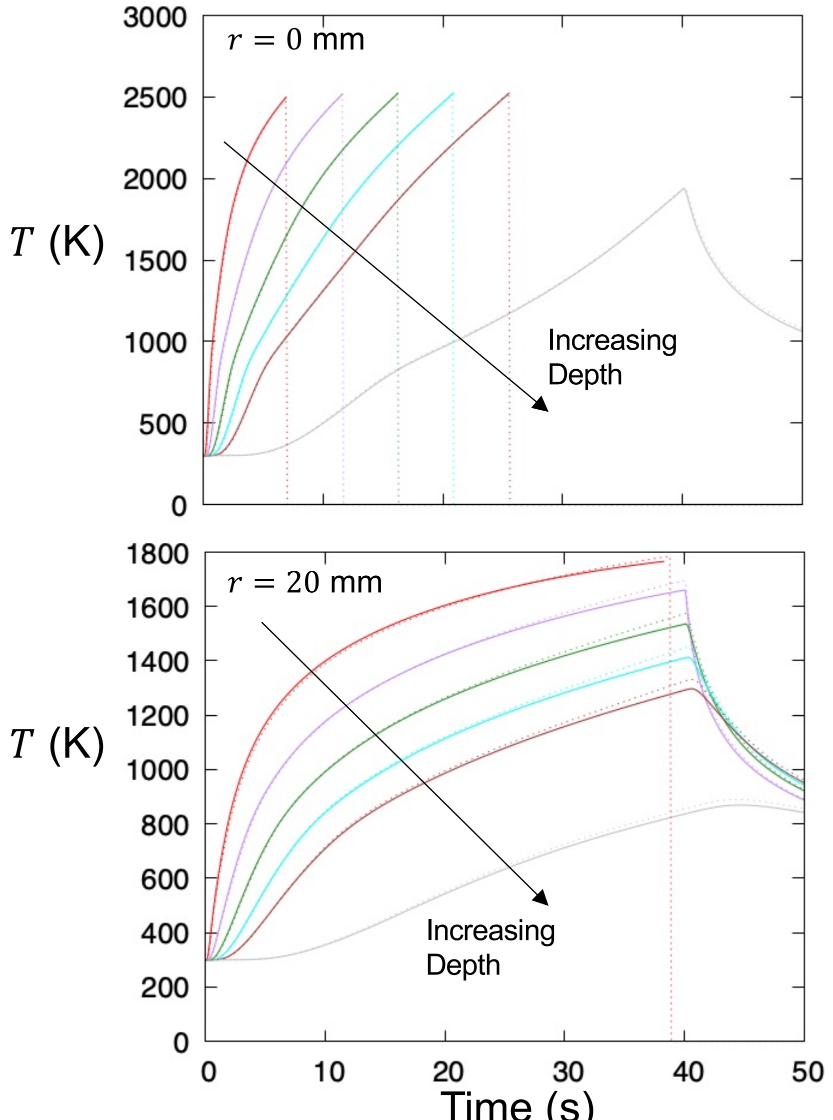

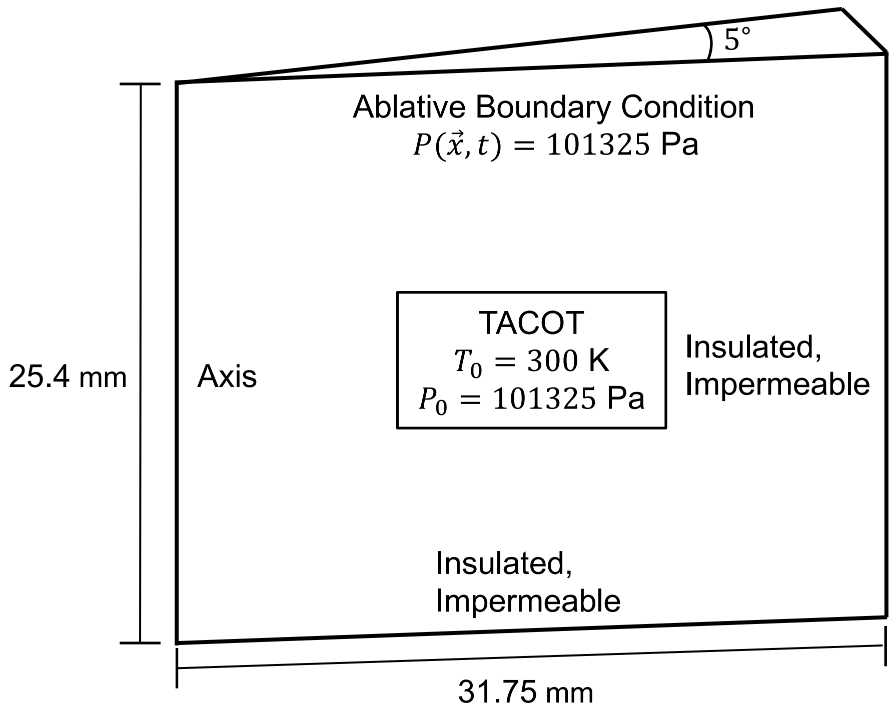
5°
Ablative Boundary Condition
$P(\vec{x}, t) = 101325$ Pa
25.4 mm
Axis
TACOT
$T_0 = 300$ K
$P_0 = 101325$ Pa
Insulated,
Impermeable
Insulated,
Impermeable
31.75 mm

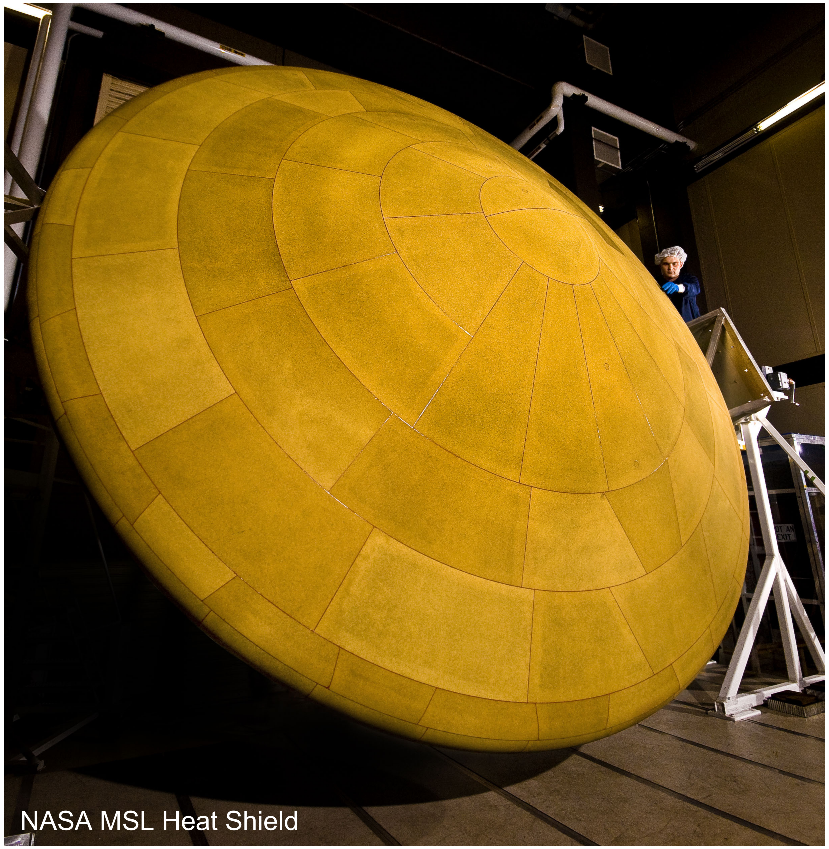
NASA MSL Heat Shield

High-Order Solutions

10 element $p = 3$ solution compared to 100 element $p = 1$
3.67x faster time to solution

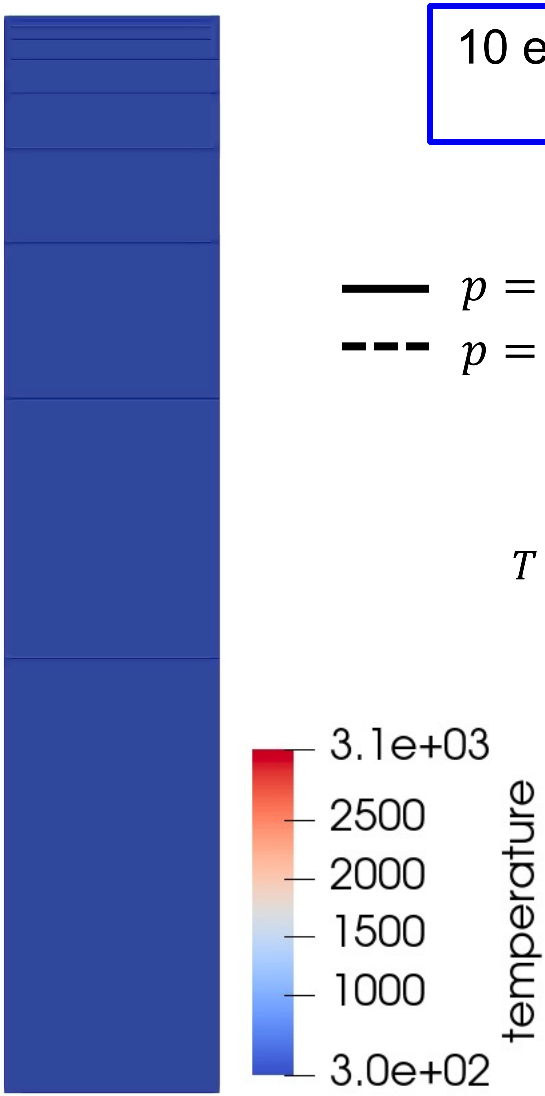

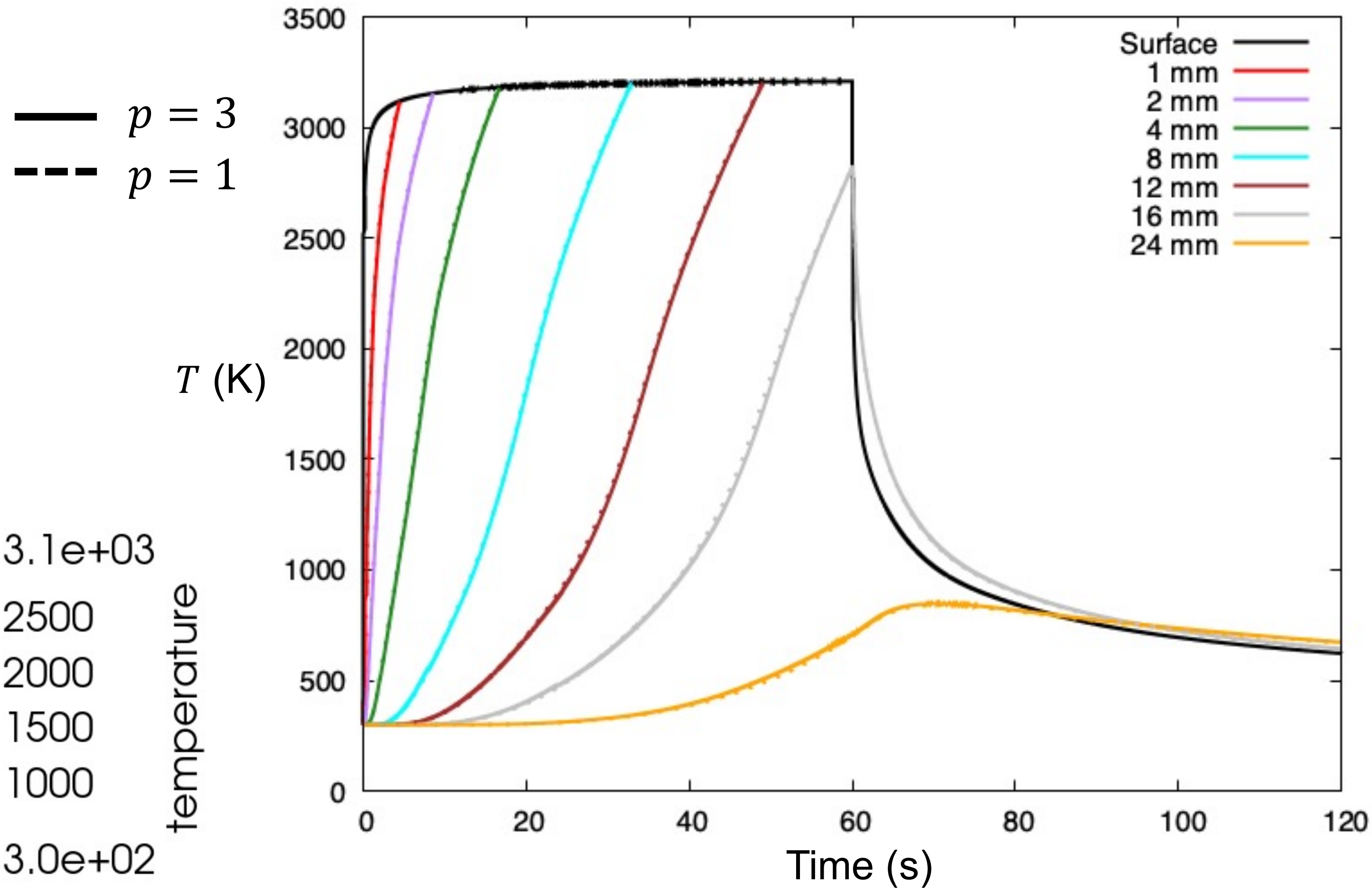

High-Order Meshes

Boundary Condition:

$$\rho U_e C_H = \frac{0.3(R - x)}{2R}$$

$$h_e = 1.5\,\frac{\mathrm{MJ}}{\mathrm{kg}}$$

$$P = 101325\ \mathrm{Pa}$$

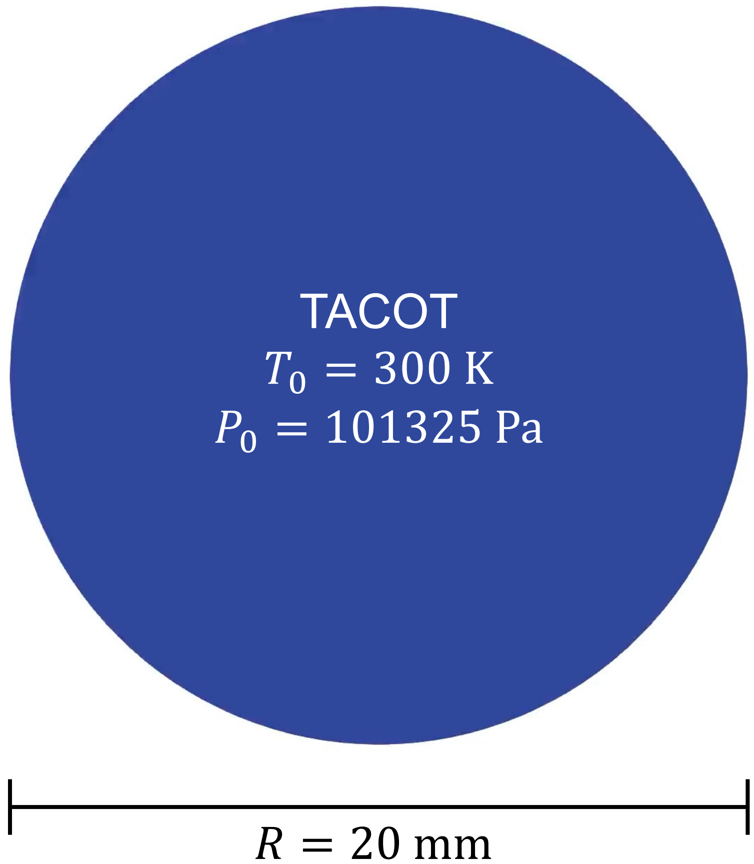

High-Order Meshes

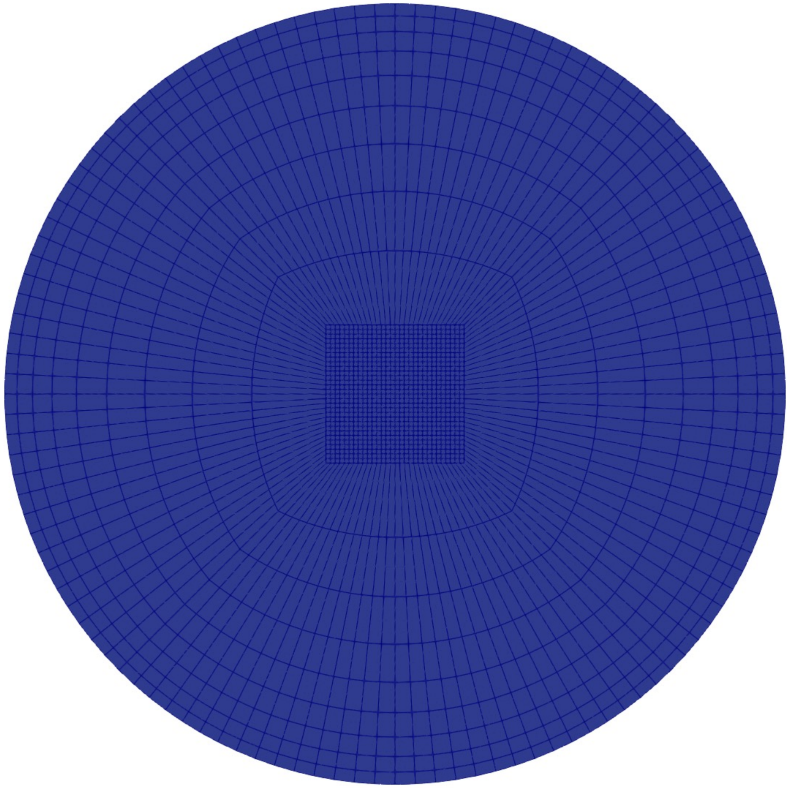

Refined Linear Mesh
2100 Elements

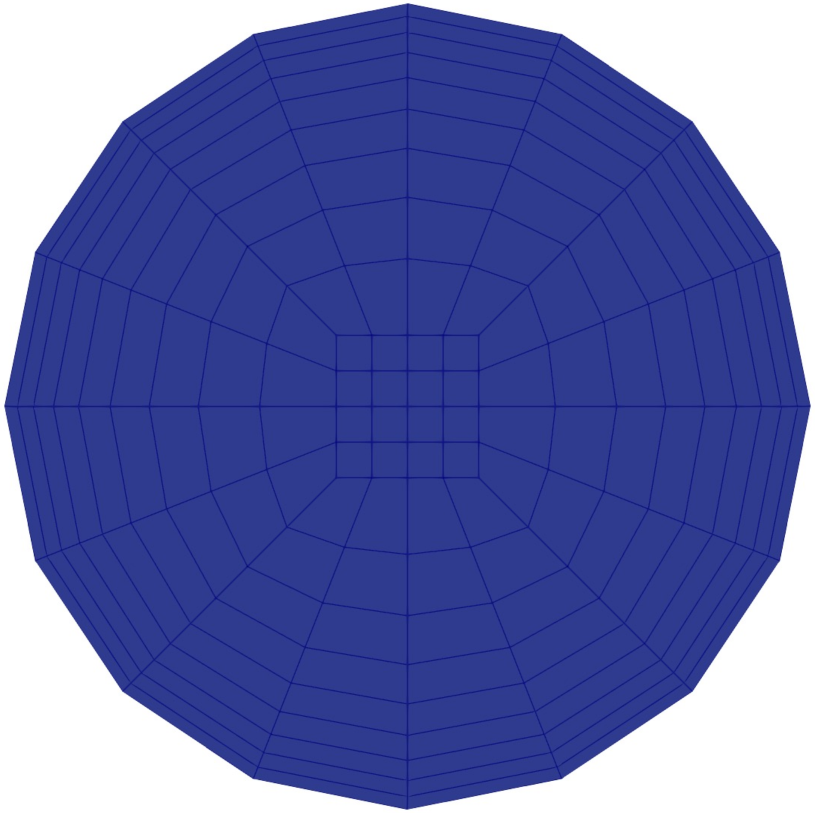

Coarse Mesh (Linear)
176 Elements

High-Order Meshes

Not to scale

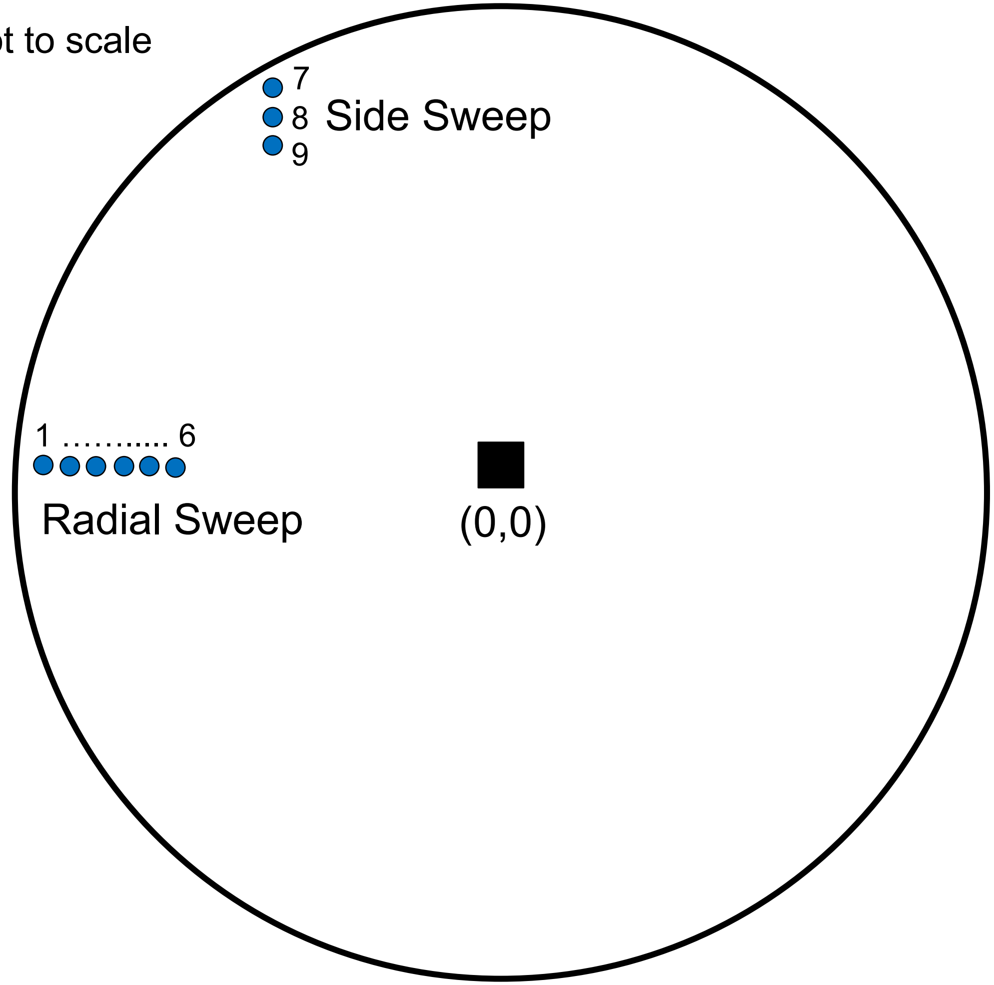

Probe	x (mm)	y(mm)
1	-9.50	0.0
2	-9.25	0.0
3	-9.00	0.0
4	-8.75	0.0
5	-8.50	0.0
6	-8.25	0.0
7	-7.07	6.82
8	-7.07	6.57
9	-7.07	6.32

High-Order Meshes

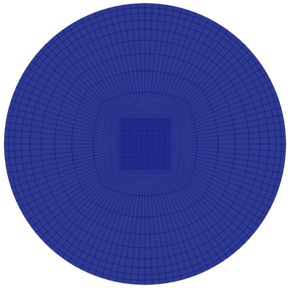

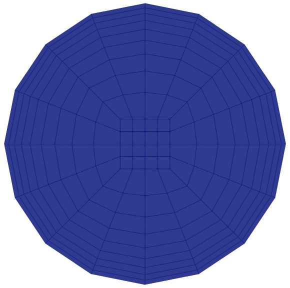

Radial Sweep

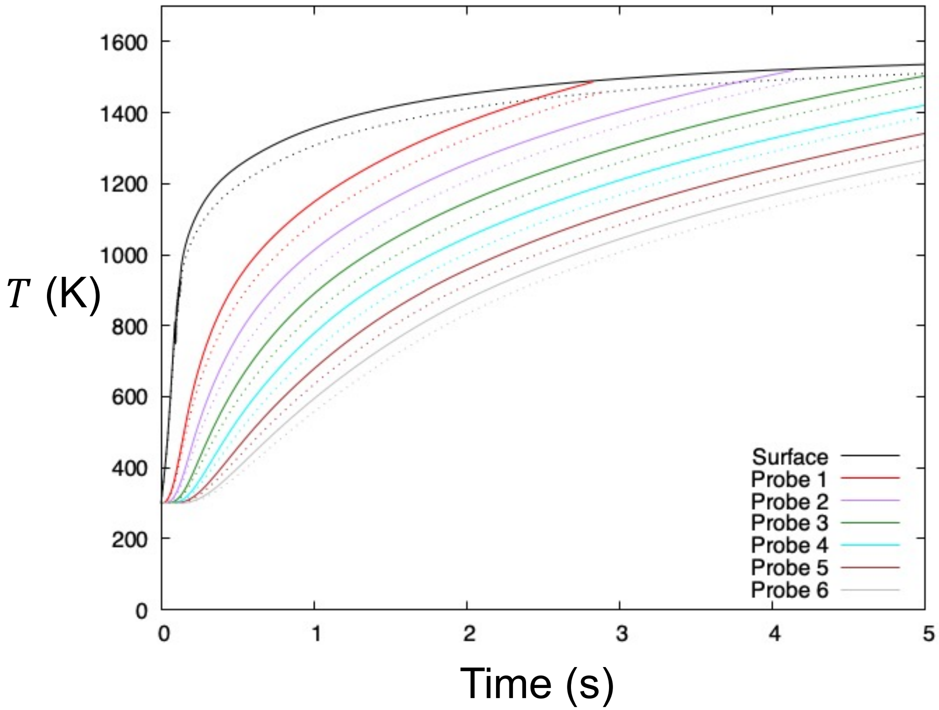

Side Sweep

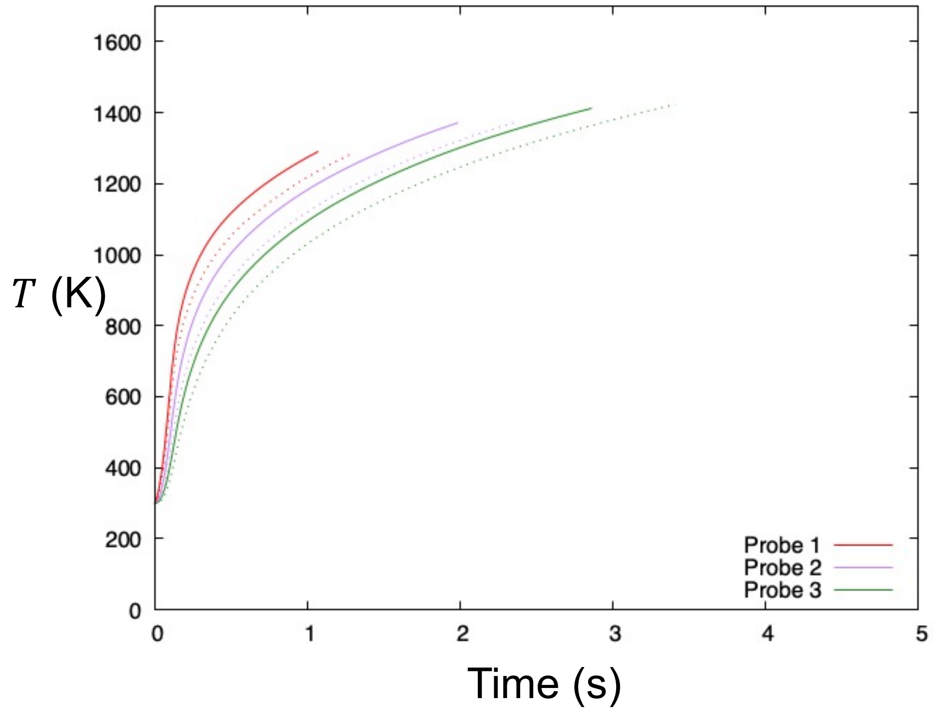

—— Coarse Linear Mesh

- - - Refined Linear Mesh

Both use $p = 2$ for internal solution

High-Order Meshes

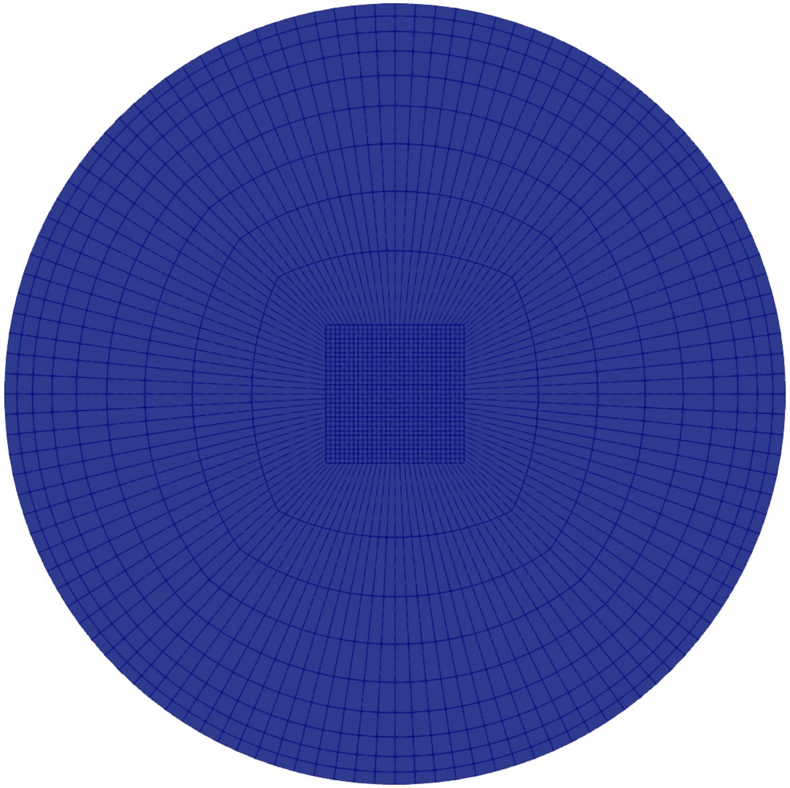

Refined Linear Mesh
2100 Elements

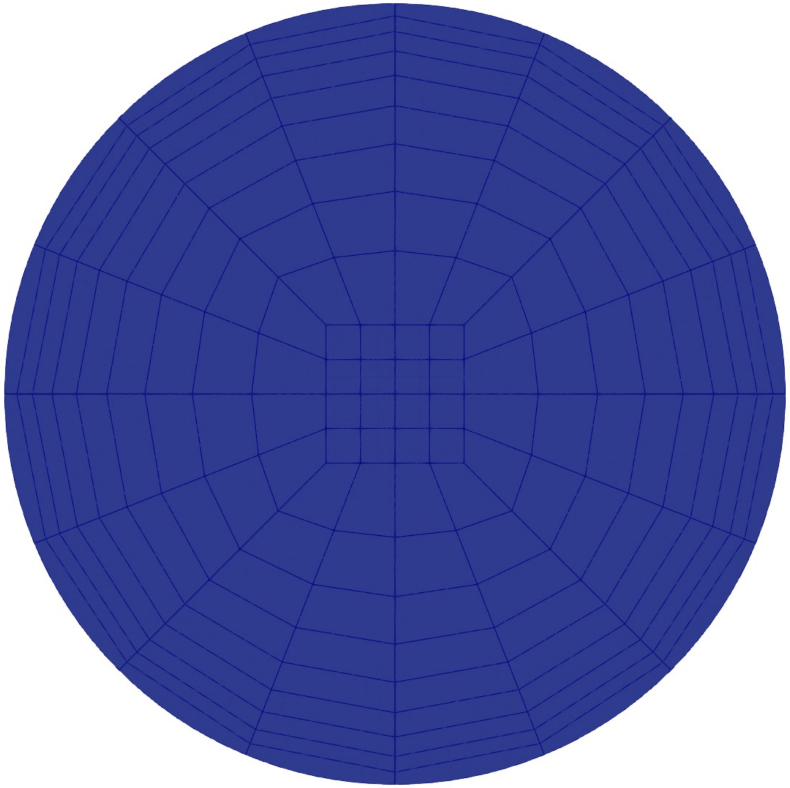

Coarse Mesh (Quadratic)
176 Elements

High-Order Meshes

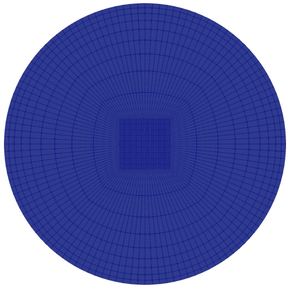

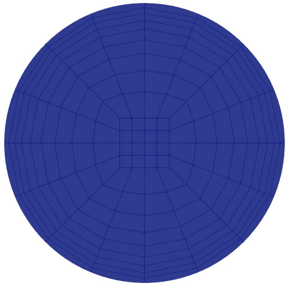

Radial Sweep

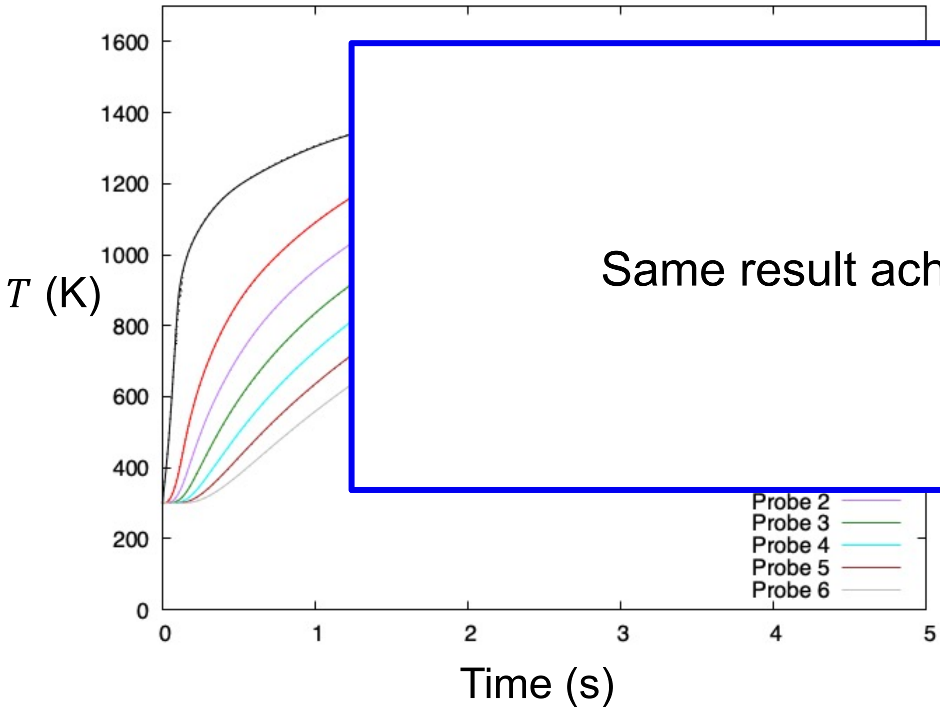

Side Sweep

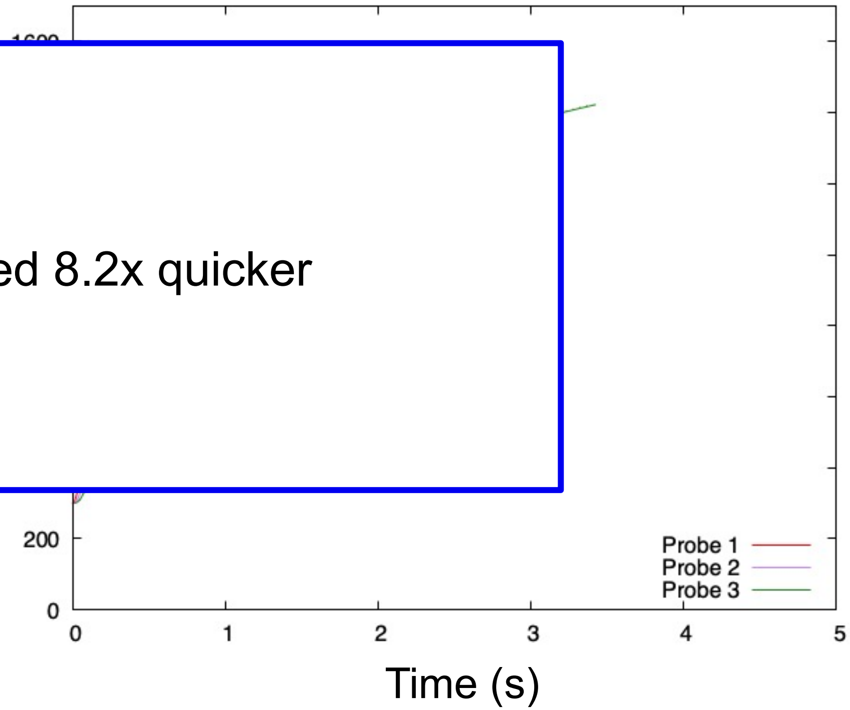

Same result achieved 8.2x quicker

Coarse Quadratic Mesh

Refined Linear Mesh

Both use $p = 2$ for internal solution

CHESS
CENTER FOR HYPERSONICS & ENTRY SYSTEMS STUDIES

Future Work

Coupling with External Flow Solvers

Mini-Arc Jet Case

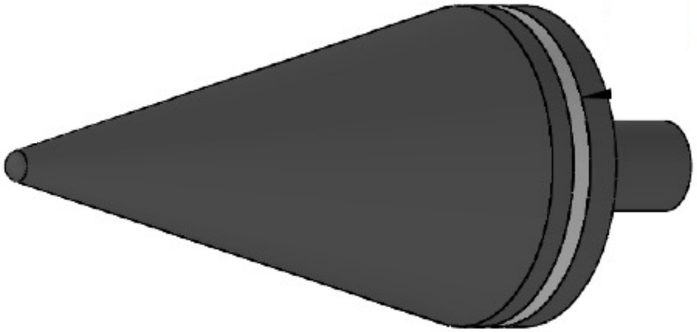

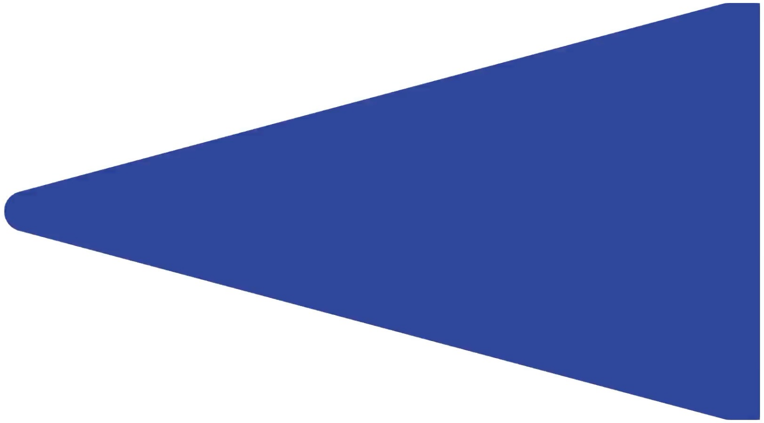

Future Work

Coupling with External Flow Solvers

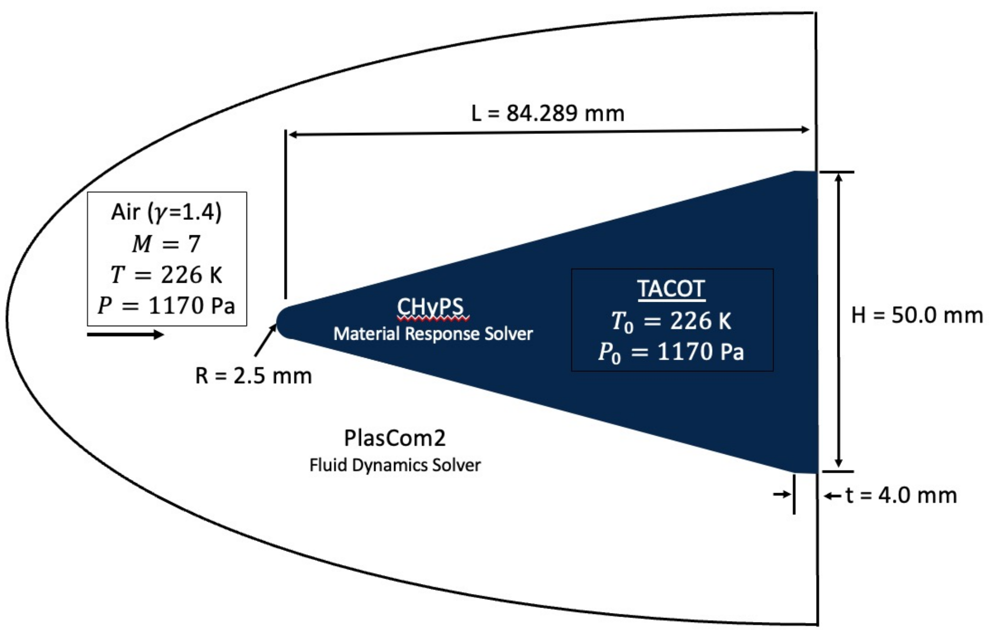

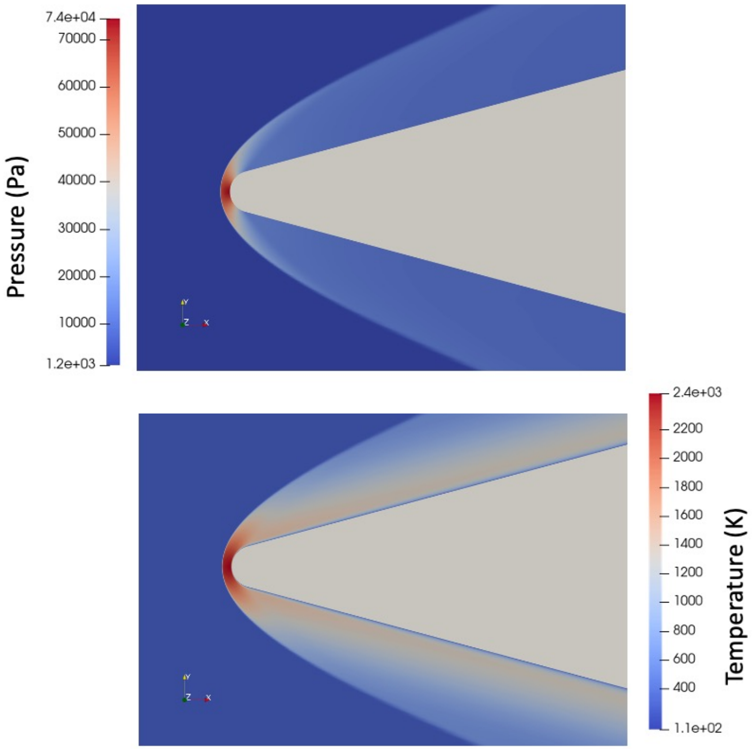

Use PlasCom2 to generate the external flow solution

Future Work

Coupling with External Flow Solvers

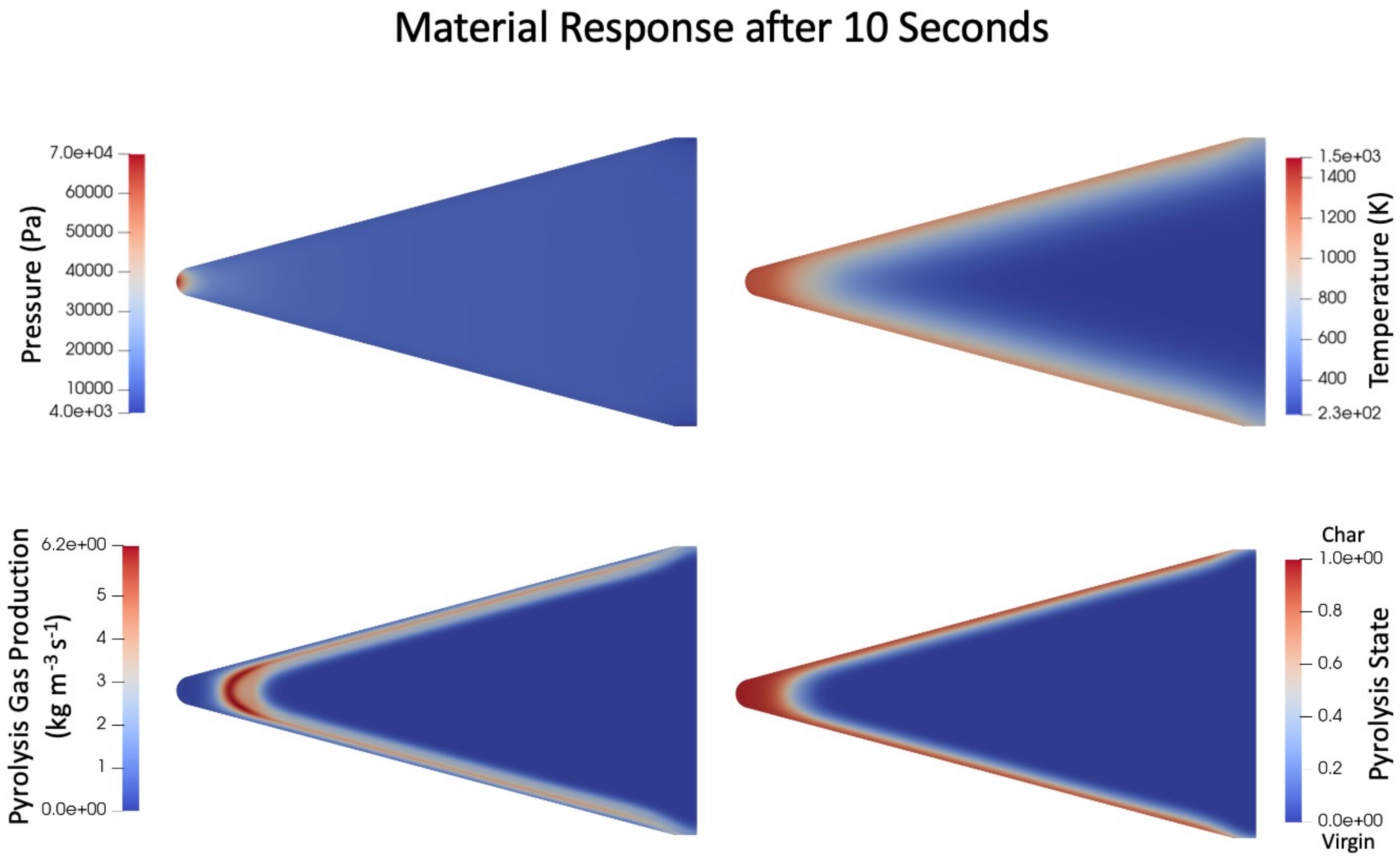

CHESS
CENTER FOR HYPERSONICS & ENTRY SYSTEMS STUDIES

Future Work

Internal Radiation using P1 Approximation

$$\frac{1}{3\kappa}\nabla\cdot\left(\frac{1}{\beta-\frac{A_1\sigma_s}{3}}\nabla G\right)-G=-4\pi I_b,\qquad -\frac{2-\epsilon}{\epsilon}\frac{2}{3\beta-A_1\sigma_s}\hat{\boldsymbol{n}}\cdot\nabla G+G=4\pi I_{bw}$$

$$\boldsymbol{q}=-\frac{1}{3\beta-A_1\sigma_s}\nabla G$$

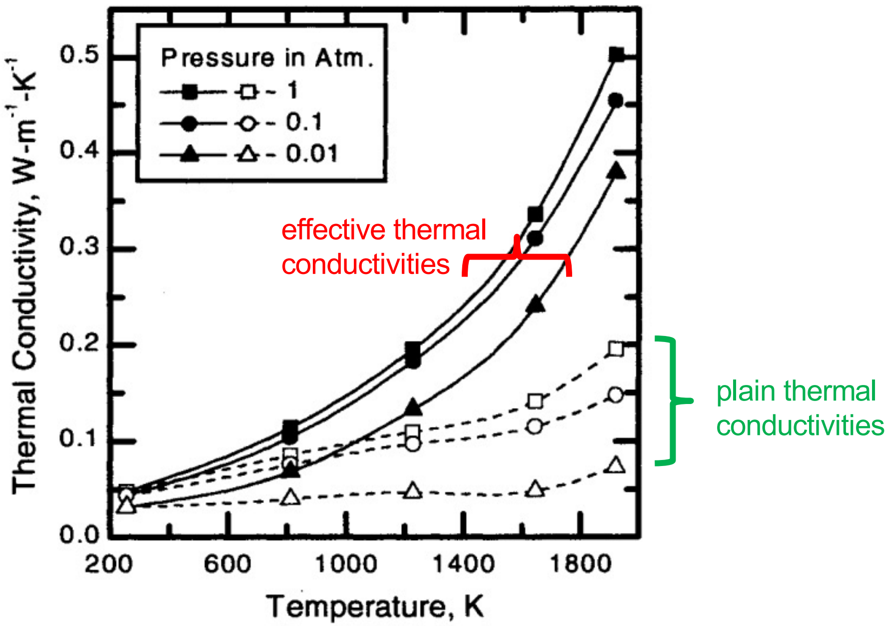

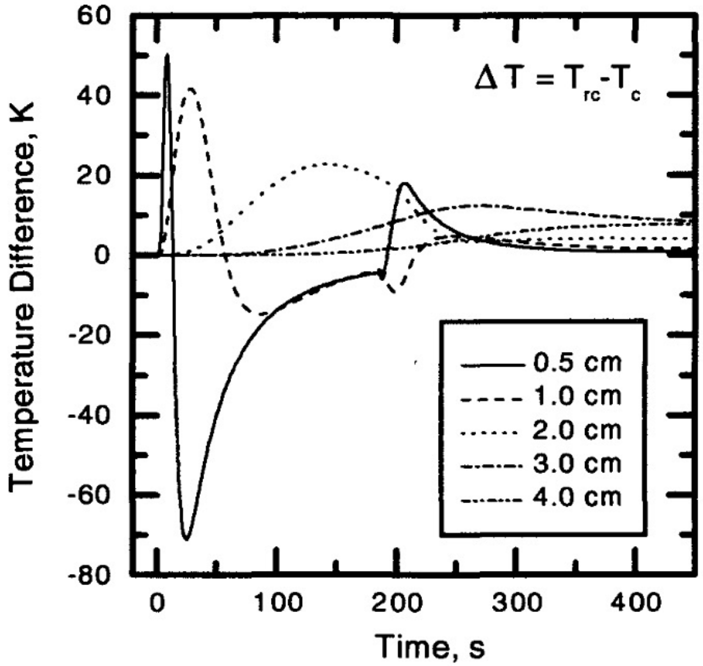

[1] Modest & Mazumder. Radiative Heat Transfer. 2021
[2] Marschall et al. AIAA Thermophysics. 2001

CHESS
CENTER FOR HYPERSONICS & ENTRY SYSTEMS STUDIES

Future Work

Insulation Estimation for Experimental Samples

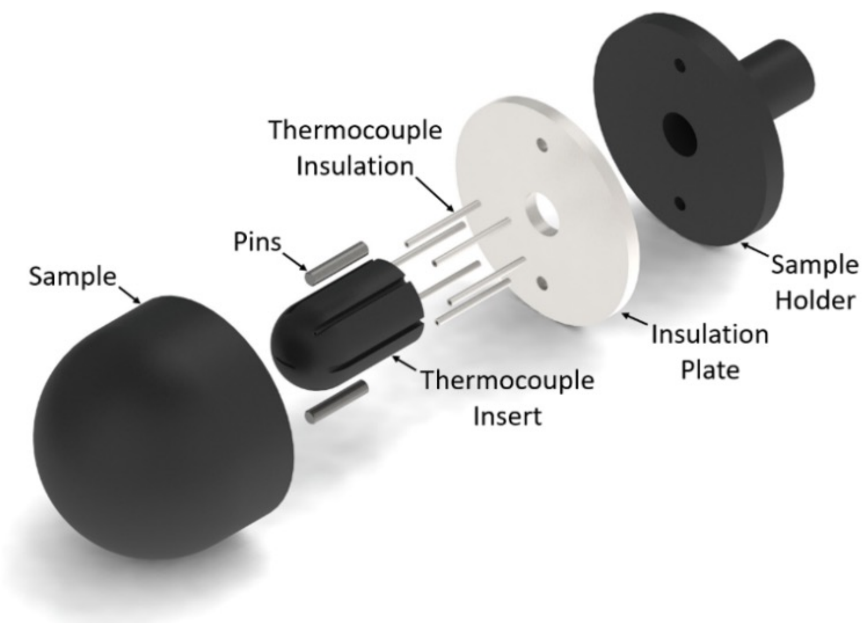

Cross-section after
10 s of heating

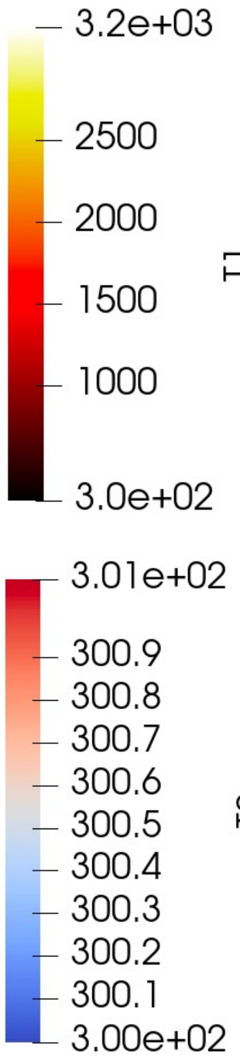

Conclusions

- Design of next-generation thermal protection systems and hypersonic vehicles will benefit greatly from computational studies
- Macroscopic volume averaged approach to simulating reactive porous materials aimed at enabling full-vehicle simulations
- Code-to-code comparison has been performed against NASA's PATO code
- Continued work will be done to leverage use of high-order solutions

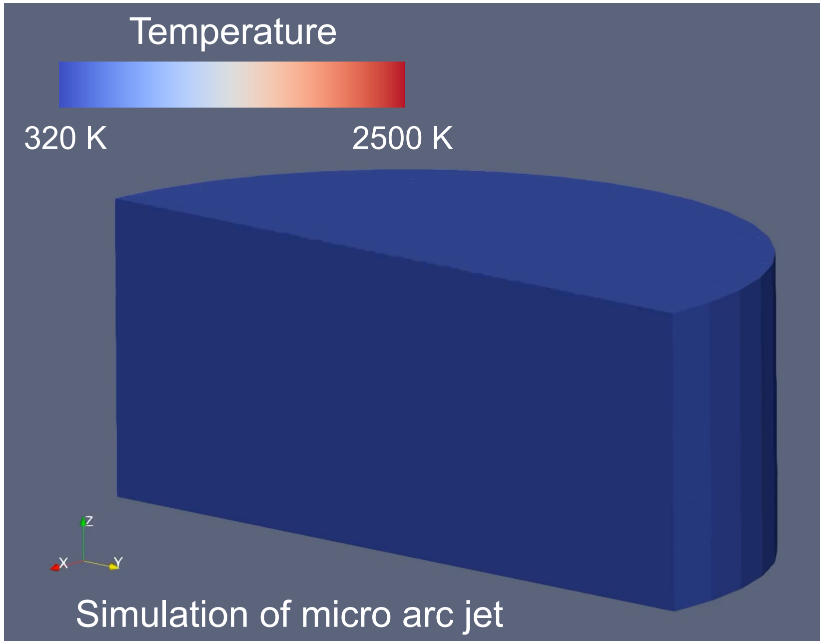

Simulation of micro arc jet